FOOD SPOILAGE MONITORING USING CARBON NANODOTS AND UV IRRADIATION REINFORCED COLORIMETRIC FISH GELATIN FILMS

A THESIS SUBMITTED TO
THE GRADUATE SCHOOL OF NATURAL AND APPLIED SCIENCES
OF
MIDDLE EAST TECHNICAL UNIVERSITY

BY

MÜNEVVER BEYZA KILIÇ

IN PARTIAL FULFILLMENT OF THE REQUIREMENTS
FOR
THE DEGREE OF MASTER OF SCIENCE
IN
FOOD ENGINEERING

SEPTEMBER 2022

Approval of the thesis:

FOOD SPOILAGE MONITORING USING CARBON NANODOTS AND UV IRRADIATION REINFORCED COLORIMETRIC FISH GELATIN FILMS

submitted by **MÜNEVVER BEYZA KILIÇ** in partial fulfillment of the requirements for the degree of **Master of Science** in **Food Engineering, Middle East Technical University** by,

Prof. Dr. Halil Kalıpçılar
Dean, Graduate School of **Natural and Applied Sciences**   _____

Prof. Dr. Serpil Şahin
Head of the Department, **Food Engineering, METU**   _____

Assist.Prof.Dr. Leyla Nesrin Kahyaoğlu
Supervisor, **Food Engineering, METU**   _____

Prof.Dr. Servet Gülüm Şumnu
Co-Supervisor, **Food Engineering, METU**   _____

Examining Committee Members:

Prof. Dr. Serpil Şahin
Food Engineering, METU   _____

Assist.Prof.Dr. Leyla Nesrin Kahyaoğlu
Food Engineering, METU   _____

Prof.Dr. Servet Gülüm Şumnu
Food Engineering, METU   _____

Prof. Dr. Behiç Mert
Food Engineering, METU   _____

Prof. Dr. İsmail Hakkı BOYACI
Food Engineering, Hacettepe University   _____

Date: 02.09.2022

iv

I hereby declare that all information in this document has been obtained and presented in accordance with academic rules and ethical conduct. I also declare that, as required by these rules and conduct, I have fully cited and referenced all material and results that are not original to this work.

Name Last name : Münevver Beyza Kılıç

Signature :

ABSTRACT

FOOD SPOILAGE MONITORING USING CARBON NANODOTS AND UV IRRADIATION REINFORCED COLORIMETRIC FISH GELATIN FILMS

Kılıç, Münevver Beyza
Master of Science, Food Engineering
Supervisor: Assist.Prof.Dr. Leyla Nesrin Kahyaoğlu
Co-Supervisor: Prof.Dr. Servet Gülüm Şumnu

September 2022, 79 pages

Foodborne diseases can lead to serious health and economic losses. Therefore, research priority has been given to the efforts to ensure food safety in recent years. Within this framework, effective and user-friendly smart packaging technologies need to be developed and integrated into food packaging applications. The proposed project aims to develop a biocompatible colorimetric film that can be integrated into food packaging where the consumer can easily obtain a real-time freshness assessment of food. Fish gelatin (FG) will be used as support material in colorimetric film fabrication. Despite the poor mechanical properties of FG, it can be produced more economically compared to the other types of gelatins. One of the main objectives of the proposed project is to strengthen the crosslinking structure of FG using carbonyl functionalized carbon nanodots (C-dots). The C-dots obtained through the pyrolysis of citric acid will be used for the chemical crosslinker, and ultraviolet irradiation will be used to improve the crosslinking structure of FG as a physical crosslinker. The effect of these crosslinkers on the barrier, mechanical, structural, and optical properties of FG films was investigated. The integration of C-

dots with UV irradiation improved these properties. In the structure of the colorimetric film, natural color pigment anthocyanins, which can be obtained by extraction from red cabbage, will be used as the sensing biomolecule. The working principle of a colorimetric film is based on a color change that anthocyanins pigments exhibit to change in the concentration of the total volatile basic nitrogen gases that release during food spoilage. The kinetic colorimetric responses of FG films against ammonia gases were investigated to simulate the spoilage of chicken breast and determine the ammonia sensitivity of FG films. UV-treated FG films containing 100 mg/l C-dots (FG-UV-100) indicated the best physicochemical and colorimetric properties. Consequently, the color change of FG-UV-100 films was correlated with microbial growth and total volatile basic nitrogen (TVB-N) release during the 9-day storage of chicken breast samples at 4°C. The main objective of this study was to identify the appropriate methods and to integrate fish gelatin and C-dots into smart packaging systems to expand their usage areas and turn them into higher value-added products.

Keywords: Fish gelatin, Carbon dots, UV irradiation, Anthocyanins, Colorimetric Films

ÖZ

GIDA BOZULMASININ TAKİBİNDE KARBON NANONOKTALARI VE UV RADYASYON İLE KUVVETLENDİRİLMİŞ KOLORİMETRİK BALIK JELATİNİ FİLMLERİNİN KULLANILMASI

Kılıç, Münevver Beyza
Yüksek Lisans, Gıda Mühendisliği
Tez Yöneticisi: Assist.Prof.Dr. Leyla Nesrin Kahyaoğlu
Ortak Tez Yöneticisi: Prof.Dr. Servet Gülüm Şumnu

Eylül 2022, 79 sayfa

Gıda kaynaklı hastalıklar ciddi sağlık ve ekonomik kayıplara yol açabilmektedir. Bu nedenle, son yıllarda gıda güvenliğinin sağlanmasına yönelik yapılan çalışmalara öncelik verilmeye başlanmıştır. Bu kapsamda etkili ve kullanıcı dostu akıllı paketleme teknolojilerinin geliştirilerek gıda ambalaj uygulamalarına entegre edilmesine ihtiyaç duyulmaktadır. Yapılan çalışmanın amacı tüketicinin kolaylık ile gıdanın gerçek zamanlı tazelik durum değerlendirmesini elde edebileceği ve gıda ambalajlarına entegre edilebilecek biyouyumlu bir kolorimetrik film geliştirmektir. Kolorimetrik film yapımında destek malzemesi olarak balık jelatini kullanılacaktır. Zayıf mekanik özellik göstermesine rağmen balık jelatini, diğer jelatin türlerine kıyasla, dini veya sağlık problemleri riski olmadan daha ekonomik üretilebilir. Yapılan çalışmanın temel amaçlarından biri balık jelatininin çapraz bağ yapısını yüzey karboksil fonksiyonlu karbon nanonoktaları kullanarak kuvvetlendirmektir. Sitrik asitten ısıl bozulma (pyrolysis) sonucu elde edilecek karbon nanonoktaları çapraz bağ yapıcı olarak (kimyasal olarak) ultraviyole radyasyon ile beraber (fiziksel olarak) ilk kez balık jelatinin çapraz bağ yapısını kuvvetlendirmek için kullanılacaktır. Çalışmada bu bağ yapıcıların balık jelatini filmlerinin bariyer,

mekanik, yapısal ve optik özellikleri üzerine etkisi araştırılmaktadır. Çalışma sonucunda Uv radyasyon ile karbon nanonoktaların entegrasyonu bu özellikleri geliştirdiği gözlemlenmiştir. Kolorimetrik filmin yapısında algılayıcı biyomolekül olarak kırmızı lahanadan ekstraksiyon ile elde edilebilen doğal renk pigmenti antosiyanin kullanılacaktır. Kolorimetrik filmin çalışma prensibi antosiyanin pigmentlerinin gıdaların bozulması sürecinde oluşan toplam uçucu bazik azot gazlarının artmasına gösterdikleri renk değişimine dayanır. Balik jelatini filmlerinin amonyak gazlarına karşı kinetik kolorimetrik tepkileri, tavuk göğsünün bozulmasını simüle etmek ve balık jelatini filmlerinin amonyak duyarlılığını belirlemek için araştırıldı. Bu çalışma sonucunda 100 mg/l carbon nanonokta (FG-UV-100) içeren UV ile işlenmiş balık jelatini filmleri en iyi fizikokimyasal ve kolorimetrik özellikleri göstermiştir. Sonuç olarak, FG-UV-100 filmlerinin renk değişimi tavuk göğsü örneklerinin 4°C'de 9 günlük depolanması sırasında mikrobiyal büyüme ve toplam uçucu bazik nitrojen (TVB-N) salınımı ile korelasyon gösterdi. Bu çalışmanın genel hedefi uygun metotları tespit ederek balık jelatini ve karbon nanonoktalarının akıllı paketleme sistemleri içerisine entegrasyonunu sağlayarak kullanım alanlarını genişletmek ve katma değeri çok daha yüksek ürünler haline dönüştürebilmektir.

Anahtar Kelimeler: Balık jelatini, Carbon nokta, UV Işıma, Antosiyanin, Kolorimetrik Film

To my family

ACKNOWLEDGMENTS

TABLE OF CONTENTS

xiv

LIST OF TABLES

TABLES

LIST OF FIGURES

FIGURES

CHAPTER 1

INTRODUCTION

1.1   Foodborne diseases and their results

Foodborne diseases originate from the consumption of food contaminated by pathogenic bacteria, viruses, or parasites (Adley & Ryan, 2016). Generally, foodborne diseases might cause mild symptoms such as diarrhea, abdominal cramp, and vomiting. However, some symptoms can be life-threatening, especially for pregnant women, immunocompromised, and/or elder people (CDC, 2019). United States (US) and European Union (EU) have taken precautions and implemented regulations through Food and Drug Administration (FDA), the US Centers for Disease Control and Prevention (CDC), and European Food Safety Authority (EFSA) to minimize the number of outbreaks. Globally 600 million people are estimated to fall sick from consuming contaminated food, which results in 420,000 deaths every year (WHO, 2015). According to CDC, foodborne diseases affect 48 million people, with 128,000 hospitalization and 3,000 deaths each year in the US (CDC, 2020). Similarly, 23 million people get sick, and 4,700 die annually in Europe (WHO, 2019). The burden of foodborne diseases cannot be only measured by the loss of health and the number of deaths. Another burden comes from the adverse effects of foodborne diseases on both economies of countries and individuals. The economic burden is caused by the productivity loss of absenteeism, health care costs, and individual income loss (Forsythe, 2020). According to the USDA Economic Research Service (ERS), 15 leading food pathogens are estimated to cause over $15.5 billion as an annual economic loss in the US (Hoffmann, Maculloch, & Batz, 2015). Overall, foodborne diseases causing health and economic loss affect millions

1

of people. Therefore, new techniques are being explored to decrease the number of outbreaks effectively and, thereby, all corresponding losses.

1.2   Food packaging

Food packaging plays an essential role in the protection of food properties such as quality and appearance. It aims to maintain these properties after the process-line during long-distance traveling and storage. In addition, the prevention of microbial and cross-contamination is another benefit of food packages. Further, the food waste due to transportation damages is decreased thanks to the protection provided by packages. Another benefit of packages is to attract the consumer to increase sales.

There are some requirements that the legislation should determine for prepackaged food labeling. According to EU 2011 Regulations, the label of prepacked foods should convey the following information: an ingredient list highlighting the allergens that food contains, storage conditions, nutrition facts per serving, and use by or best before date. Although the primary purpose of food labeling for the food industry and legislation is to inform and lead the consumer correctly, the correct perception of the labels must be the essential goal. Product date labels on traditional packages confuse the consumer about the food condition. There are many statements about the expiry date of the product, such as date of manufacture, best before date, and use-by date. These terms are standardized to avoid ambiguity among consumers or retailers about date labels. According to Codex Alimentarius (2018), "Date of manufacture" indicates the date which defined product came into existence, "Best before date" means before the date stated, the product is fully marketable before that day since the quality that asserted on the product retains. Although, after that day, the quality and flavor of the product decrease, the product could still be consumable if the specific storage conditions of the product are met since the "Best before date" term does not provide information about safety issues. The product has run out of time to be purchased due to safety issues after the "Use-by date," even if the storage conditions of the product are fulfilled. According to the FDA (2019), 20% of food

waste in the US is due to consumer confusion about food labels. Although some of these phrases stand for the peak of food quality until that date, consumers are suspicious about food safety and do not consume that food.

Traditionally, food packages have been designed as a passive system that provides products the protection, communication, convenience, and containment from external damages during transportation or distribution and storage (Young et al., 2020). With the world changing, consumer preferences have also been changing. Recently both improving shelf-life of foods and ensuring food quality are subjects that have been explored extensively. Therefore, food packaging is one of the most important research topics to meet consumer requirements. Recent technologies, such as modified atmosphere packaging and vacuum packaging, have been used to fulfill these new needs. However, tracking the product or its quality level in stages after packaging becomes vague during transportation and/or storage. Smart packaging is one of the new technologies that encompasses all conditions that should be improved from conventional packaging technology.

1.3   Smart Packaging

Smart packaging is defined as an improved version of the conventional packaging system to meet the demands of consumers, such as monitoring food quality (Young et al., 2020). It provides communication and interaction functionality to offer traceability and constant monitoring of food products after the production process is over (Vanderroost et al., 2014). Monitoring and displaying the condition of products and their environment allow manufacturers to control the products during the transportation and storage stages. Besides, embedded active agents or additives on food packaging help to maintain and improve the quality and the shelf-life of the products. Food packages with this functionality are called active packages. Smart packaging systems consist of active and intelligent functionalities (Beshai et al., 2020). The details of active and intelligent packaging are given below.

1.3.1 Active Packaging

Active packaging is one of the innovative techniques applied to improve and retain food quality and safety. In this sense, the active agents are integrated into the packaging matrix to increase the shelf-life (European Union, 2009; Bhargava et al., 2020). Different active agents can be used in active packaging applications to meet the new market expectations. These active agents could be categorized under two main groups, namely absorbers and emitters (Yildirim et al., 2018).

1.3.1.1 Absorbers

Oxygen scavengers, moisture scavengers, and ethylene absorbers are absorber-type active packaging systems. These systems aim to scavenge the undesired substances within the food environment that affect the product. Instead of adding active compounds into bulk food, integrating these compounds into packages and the release of them from the package increase their effectiveness. Since when these active compounds are in direct contact with food, they might have a higher affinity for some compounds in the food rather than the undesired substances, which lowers their activity. Furthermore, this also reduces the amount of active compounds required (Yildirim et al., 2018).

Oxygen scavengers react with oxygen and reduce the amount of available oxygen within the package (Dobrucka & Cierpiszewski, 2014). The presence of oxygen leads to many undesired outcomes in food systems. Oxidation of unsaturated fat, color change of fresh meats, fruits, and vegetables, enhanced microbial growth on a food surface, and unwanted odor change on bakery products are some of these outcomes (Cichello, 2015). The reasons for an increase in oxygen content of a package might be due to the permeability of the packaging material, poor sealing, or an inadequate oxygen removal method, which can involve gas flushing or packing

4

using a modified environment packaging system (Yildirim et al., 2018). Therefore, food scientists seek methods to eliminate oxygen in food packages and minimize the adverse effect of oxygen on the nutritional and sensory properties of food products.

Moisture control is another major concern for the food industry because moisture tends to promote microbial spoilage in the food by increasing the water activity of food over time (Yildirim et al., 2018). Consequently, a moisture absorber prolongs the shelf-life and maintains sensory attributes. Moisture absorbers are manufactured according to the relevant product types. Products such as meat, fish, and poultry have high water activity while drip loss is a common problem associated with improper freezing/thawing cycles. The liquid in a package is often a result of drip loss of meat due to degradation of muscle tissue, which reduces the appearance and thereby, attractiveness of the product for consumers (Gaikwad et al., 2019). Manufacturers commonly use moisture-drip absorbent pads to minimize the moisture-drip of these products (Realini & Marcos, 2014). These pads consist of polymer film sheets and superabsorbents that can absorb moisture 500 times greater than their weight (Dobrucka & Cierpiszewski, 2014). In addition, food products with low water activity, e.g., dried food products, are sensitive to moisture inside the package. Even at low relative humidity, product quality might deteriorate as a result of the change in food texture. Desiccants such as silica gels, minerals, and calcium oxide in sachets are used for these types of products (Dobrucka & Cierpiszewski, 2014).

Ethylene is a gaseous hormone responsible for the ripening of many fruits. Climacteric fruits ripening like bananas and tomatoes are controlled by this hormone after harvesting. During the post-harvesting period, the ethylene-induced ripening and senescence of the plants and other undesirable consequences such as altered sensory properties and quality of the product are prevented by removing ethylene from the packaged headspace (Brecht, 2019).

1.3.1.2   Emitters

The other type of active agent is emitters. In general, emitters release active agents to the product from the surface or the headspace of the package. Antioxidant/antimicrobial releasers, and carbon dioxide emitters, are some examples of active emitters (Yildirim et al., 2018).

The antioxidant in the food matrix or headspace of the package is used to minimize lipid oxidation. Synthetic antioxidants such as butylated hydroxytoluene (BHT) and butylated hydroxyanisole (BHA), natural antioxidants such as tocopherols and essential oils, or a combination of synthetic and natural antioxidants are studied by food scientists to prolong the food shelf life (Mexis & Kontominas, 2014).

Carbon dioxide shows an antimicrobial effect on food systems (Yildirim et al., 2018). Moreover, packaged products such as bakery, dairy, and fish are preserved with the proper level of carbon dioxide inside the package by suppressing deterioration (D. S. Lee et al., 2022). Commercially, some drip loss absorber pads have carbon dioxide emitters and antimicrobial components to provide a double function for muscle-based foods (Realini & Marcos, 2014). Carbon dioxide provides not only antimicrobial effects for packaged foods but also acts as an ethylene inhibitor. Ethylene action may be suppressed because of the competitive inhibition action of carbon dioxide (Brecht, 2019). Despite these effects of carbon dioxide, its concentration should be kept below the tolerance limit of the target product. Since it leads to undesired outcomes such as unwanted odor or color change when the set limits are exceeded (D. S. Lee et al., 2022).

Antimicrobial compounds eliminate or delay microbial growth on the surface of the food (Jung & Zhao, 2016). Many synthetic and natural antimicrobial agents are used in the food industry, such as organic acids, bacteriocins, spice extracts, and metals (Mexis & Kontominas, 2014). The migration of antimicrobial compounds into food is a significant concern among consumers and food authorities due to safety issues. Thus, the natural antimicrobial components isolated from plants, animals, and

microbiological sources are commonly used and integrated into active packaging systems (Dobrucka & Cierpiszewski, 2014)

1.3.2 Intelligent Packaging

Intelligent packaging is a type of food package that enables the consumer to monitor the quality and microbial safety up to the usage of the product. Intelligent packaging favors not only consumers but also food manufacturers. The intelligent package shows the real-time status of the product; for the manufacturers, it detects and records the state of the environment in which the food is located (Vanderroost et al., 2014). The last control is made at the factory by chemical and microbiological tests; on the other hand, there is no test to control the product at the consumption point (Ghaani et al., 2016). However, intelligent packages reduce the gap between the factory and consumption by monitoring the real-time status of the product, which might result in a reduction in food waste and food poisoning (Müller & Schmid, 2019).

The intelligent and active packages entered the industry first in Japan and now they are more widely used in Japan, Australia, and the USA than in Europe (Müller & Schmid, 2019). Later these new packaging technologies were placed in the European market by adapting the EU legislation (Restuccia et al., 2010). According to EU legislation (2009), intelligent packages are defined as a packaging system, which monitors the state of the packaged food with no transition from the packaging components to the food matrix. The intelligent packages can be considered traditional food packages with the extension of communication. Consequently, consumers and manufacturers can reach reliable information about the food during transportation, storage, and distribution. Data carriers, indicators, and sensors are three main types of technologies used in intelligent packages for the food industry (Müller & Schmid, 2019).

1.3.2.1   Data carriers

Data carriers provide follow-up to information flow on the food movement within the supply chain. Data carriers do not aim to collect information about the state of food quality but to prevent food theft, automate, and protect against counterfeiting (Azeredo & Correa, 2021). Barcodes and Radio Frequency Identification (RFID) tags are frequently applied types of data carriers for the food industry (Ghaani et al., 2016).

Products in the market generally have a barcode that identifies the product (Kilara, 2017). The barcodes are the cheapest and most popular data carrier form (Yam, 2012). They are composed of parallel spaces and bars or space and dots. This machine-readable form has been encoded to provide inventory and stock control and transfer information to a system that can control and process the data (Azeredo & Correa, 2021). The capacities of barcodes, which consist of two groups, 1-Dimensional (1D) and 2-Dimensional (2D), vary according to the type. 1D barcodes are composed of thin rectangles, lines, and spaces. Different composition of these items represents differently coded data that can be scanned under an optical scanner or barcode reader and transferred to the related system that is stored and processed (Ghaani et al., 2016). 2D barcodes allow more storage capacity than 1D barcodes. 2D barcodes encode data with different arrangements of dots, rectangles, and other shapes or matrix forms (Müller & Schmid, 2019). The data can be read with a scanner capable of scanning both two-dimension (vertical and horizontal) (Kato et al., 2010).

The RFID tags enable a more advanced way to provide traceability and product identification since these systems can transfer the information even at a long distance, and their storage capacity is greater (Müller & Schmid, 2019). The RFID system consists of three main groups. These are tag, reader, and middleware (local network, web server, etc.) parts. The reader part emits radio signals to capture the data from the tag that consists of two parts (microchip and antenna) and passes the data to the middleware part for analysis (Ghaani et al., 2016). There are two types of

tags: active and passive (Yam, 2012). The main difference between active and passive RFID tags is active tags have their battery to energy supply for microchips and broadcast signals to the reader. Conversely, the energy of passive tags is supplied by the reader part of the system (de Abreu et al., 2012)

1.3.2.2 Indicators

Indicators are applied to food packages to convey information to consumers about food properties in the packages (Azeredo & Correa, 2021). Indicators should meet some requirements to achieve the purpose of intelligent packaging. The indicators easily respond to environmental changes within the package and thereby, give information about the status of the package (de Abreu et al., 2012). Indicators work based on the presence/absence of target chemical substances, concentration change of these substances in the system, or the extent of reaction between food substances (Kalpana et al., 2019). Although the variety of indicators is wide, they can be categorized into three main groups. They can be listed as a time-temperature indicator (TTI), freshness indicator (FI), and gas indicator (Müller & Schmid, 2019).

The quality and safety of a packaged product can be affected by a temperature fluctuation during the distribution and storage period. The shelf life of a product is estimated under specific and appropriate conditions. Thereby the product shelf life is considered a fixed period. As intelligent packaging technology, TTIs are simple and inexpensive devices that can show the full or partial temperature history of the product depending on the time-temperature change (TAOUKIS & LABUZA, 1989). A mechanical, chemical, electrochemical, enzymatic, or microbiological irreversible change is the basis for TTIs working principle. This change is typically expressed as a visible response, such as a mechanical deformation, color development, or color movement (Selman, 1995; Taoukis & Labuza, 2003). Full history indicators and partial history indicators are sub-group of TTIs. While the full history indicators do not depend on the temperature threshold, the partial history is based on the

temperature threshold point of the product. If the temperature exceeds this point, the indicator will respond; otherwise, it will not.

On the other hand, the other type of TTIs gives an irreversible response to the temperature change at every point (Selman, 1995). TTIs can mimic the kinetic of the deteriorative process of the product; therefore, the product quality can be traced by the multicolor change of the TTIs (Zhang et al., 2013). With this benefit, the food industry employs the TTIs in intelligent packaging technologies to track the custody chain for a wide range of products. Examples of usage areas of this technology are frozen foods, chilled meats, seafood, and dairy products (Kalpana et al., 2019). Instead of tracing the shelf life of food with this technology, TTIs are used to monitor the real-time temperature of the product with reversible changes such as temperature indication of beverages for customers (Azeredo & Correa, 2021).

The quality of food products can be monitored with freshness indicators (FIs) by providing information about the metabolite formation due to chemical changes and microbiological growth within the packaged product (Müller & Schmid, 2019). Products can lose their quality when exposed to inappropriate conditions, or when the shelf-life of the product is exceeded. The consumer could judge the quality information of the product visually by an irreversible color change on FIs as a result of metabolites alteration within the package (Dutra Resem Brizio, 2016). Examples of these metabolites are volatile nitrogen compounds, carbon dioxide, hydrogen sulfides, and ethanol (Ghaani et al., 2016). Chicken meat that has high-protein content is a highly perishable food. Microbial and biochemical changes in food cause food freshness to decline with time. Long chainlike molecules of proteins can be broken down into amino acid residues or shorter fragments of polypeptides through the proteolytic activity of microorganisms (Rukchon et al., 2014). Later, amino acid residues can undergo oxidative deamination, decarboxylation, and desulfurization reactions. As a result of these reactions, amino acid residues can break down into simpler molecules like CO_2, H_2O, NH_3, and H_2S (Baston et al., 2008). The total volatile basic nitrogen (TVB-N) level, such as ammonia, dimethylamine, and trimethylamine, is used to indirectly detect microbial spoilage of protein-rich foods

(Castro et al., 2006; Rukchon et al., 2014; Smolander, 2003). As the TVB-N level increase over time, the pH of the package headspace also increases, and visible color response of FIs occurs (Kuswandi et al., 2014; Kuswandi, Jayus, Larasati, et al., 2012). Fresh foods, seafood, poultry, and fruits are examples of products that FIs can be used. The FIs currently used in the food industry are based on pH-sensitive dyes (Azeredo & Correa, 2021). The source of pigments used as a FI can be synthetic or natural. Synthetic pigments such as bromocresol blue, bromocresol green, methyl red, bromophenol red, and polyaniline (PANI) are commonly preferred in the food industry due to various advantages (Shao et al., 2021). These advantages include low price, high sensitivity to pH change, good stability, and a wide color spectrum (Alizadeh-Sani et al., 2020). Despite the listed advantages of synthetic pigments, the toxic and carcinogenic effects on human health and the environmental effects of synthetic pigments promote using natural pigments instead (Priyadarshi et al., 2021). Moreover, some natural pigments can also be extracted from various sources, including plants, insects, animals, microorganisms, and minerals (Vinha et al., 2018). Anthocyanins, carotenoids, betalains, and chlorophylls are the most commonly preferred natural plant pigments with a broad spectrum of color (Cortez et al., 2017)(Chavoshizadeh et al., 2020; Hu et al., 2020; Huang et al., 2014; Latos-Brozio & Masek, 2020; Liang et al., 2019; Liu et al., 2018; Musso et al., 2017, 2019; Naghdi et al., 2021; Prietto et al., 2017; Qin et al., 2020). For example, anthocyanins at different excitation states might appear red, blue, or purple, while carotenoids might show yellow, orange, or red colors. Similarly, betalains appear as red or yellow, whereas chlorophylls are green color pigments (Santos-Zea et al., 2019).

Chlorophylls are responsible for the green color of fruits and vegetables. They can be found in plants, algae, and cyanobacteria (Alizadeh-Sani et al., 2020). A chlorophyll molecule is composed of four pyrrole rings attached with a central atom of magnesium and a phytol hydrophobic group (Villaño et al., 2015). These pigments are affected by heat, light, aging, and oxygen (Santos-Zea et al., 2019). The processes such as senescence of green vegetables and thermal applications lead to chlorophyll

11

degradation. The color changes of chlorophylls are affected by pH and temperature; thereby, they can be applied to monitor temperature changes (MacIel et al., 2012).

Betalains are water-soluble nitrogen-containing pigments that can be categorized into two sub-groups. Betacyanins have red-violet color, while betaxanthins have yellow color on fruits and vegetables (Villaño et al., 2015). Further, betacyanins are obtained by condensing betalamic acid with cyclo-DOPA (cyclo-L-3,4-dihydroxyphenylalanine) or glucosyl derivatives; moreover, betaxanthins are obtained by condensing betalamic acid with amino acids or amines (Calva-Estrada et al., 2022). The color stability of betalain is affected by pH, light, heat, oxygen, and water activity (Naseer et al., 2019). The heat tolerance of betacyanin is greater than betaxanthin. Thus, betacyanin can be more stable in food processing than betaxanthin (Zin et al., 2020). Due to the heat sensitivity of betalains, cold chain products are more suitable to use them. The betalain sources are pitaya fruit, beetroot, cactus pear, and paperflower (de Oliveira Filho et al., 2022).

Carotenoids are lipid-soluble bioactive pigments extracted from fruits, vegetables, and flowers. Animals get carotenoids through their diets because carotenoids can be synthesized only by plants and microorganisms (Delgado-Vargas et al., 2000). In recent years, carotenoids stand out for their features such as bright color due to conjugated double bonds, antioxidant properties, and health benefits (Rehman et al., 2020). Although more than 700 different types of carotenoid pigments are found in nature, they can be categorized into two sub-groups, carotenes and xanthophylls, according to their chemical structure (Wrolstad & Culver, 2012). Algae and plants can naturally synthesize carotenes that consist of carbon and hydrogen (Mortensen, 2006) (Delgado-Vargas et al., 2000). Examples of frequently encountered carotenes are α- and β-carotene and lycopene (Mortensen, 2006). Besides carotenes, the other sub-group of carotenoids is xanthophylls, consisting of carbon, hydrogen, and oxygen. Lutein, zeaxanthin, α- and β- cryptoxanthin are examples of xanthophylls. Lutein gives the yellow color to the egg-yolks and animal fats. Lutein is commonly used as animal feed to enhance and stabilize the color of egg yolk (Boon et al., 2010). Carotenoids are red-orange and yellow pigments whose stability is affected by

external factors such as temperature, storage conditions, water activity, oxygen, and light (Santos-Zea et al., 2019). They display color transition when exposed to external factors such as temperature and UV irradiation. Overall, these pigments can be used as indicators to monitor the self-life of the product for intelligent packages (Latos-Brozio & Masek, 2020).

Anthocyanins are water-soluble pigments belonging to the flavonoid group. They are responsible for a wide spectrum of colors in plants, fruits, and vegetables with antioxidant and antimicrobial properties. In addition, the use of anthocyanins in intelligent packaging has been investigated by many researchers over the years (Kurek et al., 2018). The structure of anthocyanins is mostly based on aglycone anthocyanidin, which is glycosylated with sugar. These compounds are composed of two benzyl rings (A and B) and an oxygenated heterocyclic ring (C) that is bounded to A and B rings with three carbon bridges. In nature, there are more than 600 different anthocyanins (Wrolstad & Culver, 2012). The number and position of hydroxyl group and sugar or glycosidic linkage with aromatic or aliphatic acids can be shown as the reasons for the wide diversity of anthocyanins (Smeriglio et al., 2016). Despite the variety of anthocyanins, they are all derived commonly from 6 anthocyanidins: cyanidin, delphinidin, pelargonidin, peonidin, malvidin, and petunidin, as shown in Fig. 1 (Cortez et al., 2017). Plants-based extracts that contain anthocyanins can be used as freshness indicators due to their ability to exhibit a wide color spectrum upon exposure to different values. Butterfly pea, red rose, hibiscus, pomegranate seeds, grape, red cabbage, purple carrot, and purple sweet potato are natural anthocyanins sources that can be utilized as FI in intelligent packages (Singh et al., 2018). Among these anthocyanins sources, red cabbage (*Brassica oleracea var. capitata F. rubra*) is preferred for intelligent packaging studies because red cabbage anthocyanins (RCA) offer a broader color response as a result of TVB-N changes. The color stability of anthocyanins is affected by light, pH, oxygen, metallic ions, and temperature. At a strong acid medium (pH<2), flavylium cation that gives the red color to the substances is predominant, while the color of the anthocyanins turns purple at a neutral pH medium, and green-yellow colors are observed with a

further increase of TVB-N (Smeriglio et al., 2016). Color transformation with TVB-N increase makes anthocyanins a convenient option as a freshness indicator to monitor the shelf-life of products.
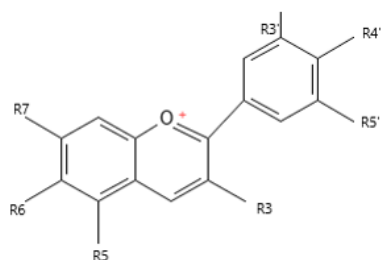
Cyanidin (Cy)	R_3 : OH	R_5 : OH	R_6 : H	R_7 : OH	R_3' :OH	R_4' : OH	R_5' : H
Delphinidin (Dp)	R_3 : OH	R_5 : OH	R_6 : H	R_7 : OH	R_3' :OH	R_4' : OH	R_5' : OH
Pelargonidin (Pg)	R_3 : OH	R_5 : OH	R_6 : H	R_7 : OH	R_3' : H	R_4' : OH	R_5' : H
Peonidin (Pn)	R_3 : OH	R_5 : OH	R_6 : H	R_7 : OH	R_3':OMe	R_4' : OH	R_5' : H
Malvidin (Mv)	R_3 : OH	R_5 : OH	R_6 : H	R_7 : OH	R_3':OMe	R_4' : OH	R_5': OMe
Petunidin (Pt)	R_3 : OH	R_5 : OH	R_6 : H	R_7 : OH	R_3':OMe	R_4' : OH	R_5' : OH

Figure 1.1. The structure of common anthocyanidin

Gas composition inside the package can vary due to the environmental conditions, among which storage conditions, the water activity of food, and package properties like permeation phenomena are crucial. Inner gas concentration can change because of food deterioration that occurs due to the biochemical activity of microorganisms over time. Gas indicators (GIs) can evaluate the efficiency of packaging components and possible leakage. Therefore, GIs inform about the package integrity throughout the entire custody chain. GIs are used to detect the microorganism activity and enzymatic reaction in the food matrix. Monitoring oxygen concentration by GIs is widely studied in the food industry (Drago et al., 2020). Oxygen concentration should be controlled in the package medium since it promotes microbial and biochemical deterioration and commonly initiates lipid oxidation. Because of this, oxygen scavengers are used to remove the oxygen from the packages. However, the bad sealing or the transportation conditions may affect the package integrity and lead

the oxygen penetration inside the package. GIs give an immediate visible response to oxygen without needed laboratory equipment. The colorimetric indicators based on redox dye are used to detect oxygen. Methylene blue is an example of redox dye to use for this purpose. Methylene blue is reduced with reducing sugar in an alkaline solution. It turns to a colorless form, and if there is oxygen, the dye is oxidized and colored (Kuswandi et al., 2011). GIs are, in general, integrated into the packaging material. Therefore, they should meet certain requirements including but not limited to being nontoxic and water-insoluble (Ghaani et al., 2016).

1.3.2.3   Sensors

Sensors are analytical devices that detect or quantify a signal that measures a certain change in physical, electrical, or chemical properties in the sensor schematic (S. Y. Lee et al., 2015). Terms of sensors and indicators are used interchangeably from time to time, although there are some distinctions. Sensors measure only certain aspects and require a separate device to transduce the sensor signals to obtain the response, while indicators, particularly colorimetric ones, can display the colorimetric response directly without a need for a transducer element (Heising et al., 2014). Sensors have two main components: the receptor unit and the transducer unit. The receptor unit is responsible for detecting certain physical or chemical analytes and transforming the physical or chemical information into a measurable energy form for the transducer unit (Kerry et al., 2006). Moreover, the transducer unit transforms this energy form into analytical signals (Azeredo & Correa, 2021). These signals can be electrical, thermal, or optical signals. Biosensors and gas sensors are the two main types of sensors that are integrated into intelligent packaging technologies. The spoilage process of packaged food can be detected by the concentration of certain gaseous. Gas sensors respond reversibly to the physical parameters of the sensor that are altered in the presence of the gaseous analyte; thereby, the food quality can be monitored by an external device (S. Y. Lee et al., 2015). Biosensors combine biological components such as enzymes, antibodies, and nucleic acids to detect and

15

analyze certain target analytes to produce measurable signals by the transducer units (Michelmore, 2016). There are some requirements for using sensors in food packages, such as selectivity for the target species, high sensitivity to this species concentration change, short response time, and long life-time (Ghaani et al., 2016).

1.4   Polymers Used in Food Packaging

Petroleum-based (synthetic polymer) packages have been widely preferred in the food industry over the past few decades because of their advantageous features. Polyethylene terephthalate (PET), High-density polyethylene (HDPE), Polyvinyl chloride (PVC), Low-density polyethylene (LDPE), Polypropylene (PP), and Polystyrene (PS) are the polymers commonly used in food packages (Tajeddin & Arabkhedri, 2020). The advantages of synthetic polymer packages can be listed as being economical, functional, mechanically tunable, and easily extrudable into any shape. Even though synthetic polymers offer many advantages, as listed above, more environmentally friendly packaging materials are in great demand due to environmental problems associated with the use of synthetic polymers. Non-degradability and pollution are the main concerns that cause environmental problems. The pollution is caused by the manufacturing process and disposal of package wastes. These concerns have driven research efforts to look into new sources for renewable and biodegradable raw materials. Biodegradable materials are defined as substances that convert into natural components such as water and carbon dioxide as a consequence of a chemical deterioration process by the enzymatic activity of microorganisms present in the environment (Salgado et al., 2021). In the food industry, environmental concerns and consumer demands for biodegradable food packages have led to excessive efforts for the use of proteins and polysaccharides as food packaging materials in the last two decades (Rhim & Ng, 2007). Biodegradable and renewable polymers can be classified into two categories (Averous & Boquillon, 2004). The first category is agro-polymers, consisting of agro resources such as polysaccharides-based (starches, pectin, and gums) and protein-

based (collagen, gelatin, soy protein, gluten) polymers. The second category is microbially produced polymers such as polyhydroxyalkanoates (PHA), and the final category is chemically synthesized polymers such as poly(lactic acid) (PLA). Biodegradable polymers can protect product quality by acting as a barrier against oxygen and water vapor permeation into the package. In some cases, they might also act as a carrier for antioxidants, antimicrobial, and colorimetric agents (Rhim & Ng, 2007).

1.4.1 Gelatin

Gelatin is a biopolymer derived by thermal denaturation of collagen that is present in animal skins and bones. It is widely used in the food, pharmaceutical, and cosmetic industries. Functional properties of gelatin, such as water-binding, gel formation, barrier, and film formation, made gelatin an appealing raw material for various industrial fields (Lu et al., 2022). Pigs and mammals are the common sources of gelatin extraction. However, religious concerns and diseases such as bovine spongiform encephalopathy (BSE) (mad cow disease) lead the food industry to search for alternative gelatin sources.

Fish gelatin (FG) is a potential alternative to bovine and porcine gelatins. Using fish tissue to obtain FG greatly reduces the waste from fish processing (Derkach et al., 2020). The good film-forming, transparency, and flexibility properties of fish gelatin provide the food industry to use it as an alternative source (Gómez-Guillén et al., 2009). FG films have some limitations, such as low tensile strength and high-water solubility because of lower amounts of proline and hydroxyproline amino acid residues than mammalian gelatin (Bae et al., 2009). Therefore, the mechanical properties of FG are poor when compared to mammalian gelatin. Cross-linking is a method to provide modification of polymers by chemical or physical methods (Cao et al., 2007). To enhance the mechanical properties of FG films, chemical and physical crosslinkers are investigated. Chemical cross-linking occurs mainly as a result of covalent bonds and intermolecular interactions. The substances employed

for this are called crosslinkers or crosslinking agents. Aldehydes have been frequently utilized as a chemical crosslinker, but due to their toxicity, alternative natural reagents are investigated (Cao et al., 2007). The functional groups of the reagents such as carbonyl, carboxyl, and hydroxyl groups react with the substances and enhance the mechanical properties. Cross-linking with fish gelatin is based on the condensation of the aldehyde and ε-amine groups found in lysine and hydroxylysine residues (Chaibi et al., 2015). Nanotechnology can work with materials with dimensions less than 100 nm to understand the material structure and create materials with new properties (Roco, 2003; Schmidt et al., 2002; Thostenson et al., 2005). It can support minimizing the problems of films with functional qualities, and applications (Dash et al., 2022). Nanoparticles have higher surface activity and surface area that favors the nanoparticle-matrix interaction. This results in improving the functionality of the final product. Therefore, the application of nanoparticles in food packages to improve their properties is searched recently (Azeredo, 2009; Dash et al., 2022; Lagarón et al., 2005; Sadeghi et al., 2021; Sorrentino et al., 2007). Nanoparticles have been studied to enhance the mechanical properties of fish gelatin as a promising option (Bae et al., 2009). Carbon dots (C-dots) are one of these nanoparticles that are utilized in food packages (Li et al., 2016; Rani et al., 2020; Roy et al., 2021; Wang et al., 2017). C-dots made from carbon sources could act as a crosslinker due to their large number of surface functional groups, such as carboxyl and hydroxyl groups (Dhenadhayalan et al., 2016). The carboxylic group can interact with the ε-amine of lysine, generating stable amide bonds.

Moreover, in terms of nontoxicity, interfacial properties, photoluminescent yield, and ease of fabrication from inexpensive precursors make C-dots prominent among other nanomaterials (Yu et al., 2019). Besides the C-dots, ultraviolet (UV) irradiation can be applied to improve mechanical properties as a physical cross-linker.

The physical or radiation cross-linking method is based on the application of an external source of high energy to create to produce intermediate excited transition state species which can decompose and create free radicals (Walsh, 2011). This

18

method has recently received increased attention due to its several advantages. Simplicity and low cost are some of these advantages (Rezaee et al., 2020). The energy that comes from irradiation creates electronically excited molecules that can cause chemical reactions in proteins, such as modification of cross-links (hydrogen bonds, ionic, and hydrophobic interactions); as a result, molecular fragmentation occurs (da Silva & Pinto, 2012). UV irradiation creates molecular fragmentation and denaturation (Anastase-Ravion et al., 2002). This causes the free radical formation of gelatin amino acids (Otoni et al., 2012). These radicals can either react with each other and lead to the covalent bond formation or react with the present compound (Char et al., 2019; Hurley et al., 2013). Moreover, among the other source of ionizing irradiation, UV irradiation has many advantages, such as ease of use and low penetration power. It is a weaker type of electromagnetic radiation than ionizing radiation, also. It has considerable potential for altering the physical and mechanical properties of protein-based films (Bhat & Karim, 2014).

1.5 Objectives of the Study

Detection and recording the state of the environment in which the food is located and monitoring the real-time product status are some advantages of intelligent packaging. Using biodegradable polymers such as gelatin in intelligent packaging applications could subside the global concerns about the growing environmental problems associated with packaging waste. Compared to its counterparts, fish gelatin has the Kosher and Halal status that meets the demand of specific religious groups while it indicates no risk of Bovine Spongiform Encephalopathy. However, its mechanical properties are exiguous. Cross-linkers can be utilized to reinforce these properties and could be achieved by adding nano-materials with the surface functional groups. In addition to chemical reinforcement, the physical technique can also be applied to improve the mechanical properties of fish gelatin. UV irradiation improves the mechanical and physical properties of the fish gelatin-based film by forming free radicals from the amino acids of FG; these radicals can be cross-linked to each other.

In literature, there are many studies about improving FG properties to be utilized in the food packaging industry. However, there is a limited (or almost none) study about the fabrication of FG film with chemical (C-dots) and physical reinforcer (UV irradiation) or both reinforcers applied.

Intelligent films doped with anthocyanins as an indicator are suitable for monitoring food quality during storage. Especially for protein-rich products such as fish, chicken spoilage changes the chemical composition of the package headspace due to releasing the TVB-N components. RCA changes the color in response to volatile amine release during spoilage. Therefore, RCA is a suitable pigment to use as an indicator for colorimetric films. There is limited number of studies on RCA doped FG films as a freshness indicator. Therefore, the objectives of the study were to fabricate a colorimetric sensor film using C-dots and anthocyanins through UV-light induced crosslinking and to evaluate the physical, morphological, and mechanical properties of these films concerning the different concentrations of C-dots.

CHAPTER 2

MATERIAL AND METHOD

2.1   Material

FG was supplied from SG Chemicals. Sodium phosphate monobasic and sodium phosphate dibasic, magnesium oxide, boric acid, and bromocresol green-methyl red indicator solution were provided from Sigma-Aldrich (St. Louis, MO). Hydrochloric acid fuming (37%), citric acid, and ammonium chloride were purchased from ISOLAB (Wertheim, Germany). Ammonium hydroxide solution (32%) was provided by Merck (Darmstadt, Germany).

2.2   Colorimetric film fabrication

2.2.1   Anthocyanin extraction from red cabbage

RCA was extracted from red cabbage according to the method described by Chandrasekhar et al. (2012). 50 g of red cabbage leaves cut into small pieces and then was macerated in 100 ml of distilled water by stirring for 24 hours at 450 rpm at room temperature. The extract was separated from the leave residues by filtering firstly through Whatman #1 and followed by a 0.45 µm syringe filter. According to the pH differential method, the RCA concentration was estimated. This method is based on the Lambert-Beer law. The absorbance of anthocyanins extracts at pH 1 and 4.5 are obtained for the wavelength at 530 nm and 700 nm. The difference in these absorbance values defines the anthocyanins concentration in the solution. Next, the RCA stock solution concentration was adjusted to 1 mg/1 in 100 mM

sodium phosphate buffer at pH 6 and stored at 4 °C in the dark for future use (FULEKI & FRANCIS, 1968).

2.2.2   C-dots synthesis

C-dots were synthesized as a result of the carbonization of citric acid with microwave energy according to the method described by Dhenadhayalan et al. (2016). In order to synthesize C-dots, 10 % (w/v) citric acid solution in distilled water was heated at 550W for 7 minutes in a microwave lab station (Ethos D Microwave Labstation, Milestone Inc., USA). During the heat treatment, the color of the sample changed from colorless to brownish yellow, and a foamy form was obtained after treatment. This residue was dissolved in distilled water and purified by dialyzing against ultrapure water with dialysis tubing (1200 Da cutoff, Sigma, D7884- 10 FT) for 48 hours. Finally, the C-dots solution was freeze-dried (Christ Alpha 2-4 LD Plus, Martin Christ, Germany). After characterization of synthesized C-dots, 1g/ml stock C-dots solution was prepared in 100 mM sodium phosphate buffer by adjusting pH 8.

2.2.3   Spectral analysis of RCA and CDs

UV-Vis spectra of RCA and C-dots solutions were obtained by UV-Vis spectrophotometer (Optizen Pop, Mecasys, Seoul, Korea). The spectra were measured in 100 mM sodium phosphate buffer in a range of 300 – 700 nm from pH 2.0 to 12.0.

2.2.4   Fish gelatin films fabrication

The solvent casting method was used to produce FG films consisting of FG, RCA, C-dots, and glycerol. The final concentrations of FG, RCA, and glycerol were adjusted to 10 % (w/v), 0.5 mg/l, and 1% (w/v), respectively. Initially, FG was

dissolved in 100 mM sodium phosphate buffer at pH 8 and stirred at 50 °C to produce a clear solution. Next, RCA and glycerol were added. Glycerol was added as the plasticizer to the precursor solution. The pH value of the prepared solutions was adjusted to 8 after adding C-dots at a final concentration of 25 mg/ l, 50 mg/ l, and 100 mg/ l. Next, the precursor solution was ultrasonicated to combine all components properly at 50 °C for 45 minutes. After preparing solutions, two different procedures were followed. First, 15 ml of solution was poured into a 9 cm in diameter polystyrene Petri dishes and placed into the 0% relative humidity desiccator with silica gels at 23°C for 48 hours. The control sample (had no C-dots) was marked as FG. The second procedure had an extra step before being placed into the desiccator. This step included the treatment of the prepared solution by irradiation with UV lights (1.5 mW/cm, 365 nm, Vilber ECX-F20.L-V1) for 45 minutes. This control sample was marked as FG-UV. Fabrication of different concentrations of C-dots (25 mg/l, 50 mg/l, and 100 mg/l) was followed the second procedure described above, and they were marked as FG-UV-25, FG-UV-50, and FG-UV-100. Before the analysis, all films were conditioned in the climate chamber (TK120, Nuve, Ankara, Turkey) at 23 °C and 52% relative humidity.

2.3   Characterization of colorimetric films

2.3.1   Mechanical and barrier characters of the FG films

A Zwick/Roell Z250 universal testing machine (Ulm, Germany) was used to assess the mechanical properties of the developed films. For this part of the study, the solvent casting method was applied to 12 x 12 cm square Petri dishes during film fabrication.

Tensile strength measurements were performed with films that were cut with a manual cutting press (ZCP 020, Zwick GmbH&Co., Ulm, Germany) into a special dog bone shape (a gauge length of 25 mm and a width of 4 mm). Tecnair LV climatic room conditioner was used to maintain the temperature and relative humidity of the

testing environment at 24 ± 1 °C and 51 ± 1 %, respectively. The samples were placed between the pneumatic grips with an initial gap of 20 mm and pulled apart at a crosshead speed of 50 mm/min. The testXpert software was used to estimate the tensile strength (TS) and percent elongation at break (EAB). TS was calculated by the formula that the ratio of maximum load before the rupture to the cross-sectional area of the films. EAB was calculated with the ratio of the measured value of length till the rupture of films and the initial length.

The Mchugh et al. (1993) approach was applied to determine the water vapor permeability (WVP) of films. WVP was assessed as g / m.s.Pa. The thickness of the films was measured using a digital micrometer (LOYKA 5202–25, Loyka, Ankara, Turkey) at seven different locations. 35 ml water was added to the cylindrical cups that had a 4 cm internal diameter to achieve 100% RH. The cups and their caps were positioned to squeeze the films between them. After the initial weights of the cups were recorded, the cups were placed into a desiccator with silica gels. The changes in the desiccator's inner temperature and relative humidity, as well as the weight of cups, were recorded for 12 h at 1h intervals.

2.3.2   The water solubility of the FG films

The films were weighted after being cut into pieces for measurement of moisture content. Then the films were dried at 105 °C until the constant weight was attained. Eq. 1 was used to calculate the percentage of moisture content (MC%)

$$\% \, \mathrm{MC} = \frac{W_0 - W_1}{W_1} \times 100 \qquad\qquad (1)$$

where w_0 was the initial weight and w_1 was the weight after drying.

GONTARD et al. (1994) technique was slightly modified in order to determine the water solubility (WS) of films. The 2 x 2 cm pieces were submerged in 50 ml distilled water and stored at room temperature for 24 hours. With the help of the filter paper,

excess water was removed, and the films were dried at 105 °C till they reached their constant weight (W_2). WS was calculated according to Eq. 2

$$WS = \frac{W_0\left(1-\%\frac{MC}{100}\right) - W_2}{W_0(1-\%\frac{MC}{100})} \times 100 \qquad (2)$$

2.3.3 Thermal properties of FG films

The differential scanning calorimeter (DSC) (Perkin Elmer, DSC 4000, CT, USA) was used to determine the thermal properties of films. Each film sample was dried for 48 hours in a vacuum oven at 40 °C. Then they were weighed into an aluminium pan (5 mg) and sealed. The temperature range of the scanning was between 20 and 120 °C with a heating rate of 10 °C/min under inert nitrogen gas. The empty sealed pan was taken as a reference during the scanning.

2.3.4 Structural analysis

The high-resolution transmission electron microscope (HRTEM) (FEI, Tecnai G2 Spirit Biotwin, Oregon, USA) was used to examine the surface morphology of C-dots while operating at an accelerated voltage of 20–120 kV. Scanning Electron Microscope (FESEM) (FEI, QUANTA 400F Field Emission SEM, Oregon, USA) with 5 kV accelerating voltage was used to investigate the cross-sectional morphologies of the films. All film samples were cryofractured for FESEM analysis. The attenuated total reflection Fourier transform infrared spectroscopy (ATR-FTIR) SHIMADZU, IRSpirit, Kyoto, Japan) was used to examine the interactions and alterations of chemical bonds of C-dots, RCA, and films in transmission mode with the range of 4000- 750 cm^{-1} at 4 cm^{-1} resolution properties. The crystallinity of C-dots and fish gelatin films was analyzed by an X-ray diffractometer (XRD) (Rigaku, MiniFlex XRD, Tokyo, Japan). XRD measurements were performed at 2θ with the range of 10° to 70° for C-dots and 5° to 55° for films. The C-dots were freeze-dried

before the experiment. The percent relative crystallinity (X_c) was calculated with Eq.3

$$Xc = \frac{A_c}{A_c - A_a} \times 100 \qquad (3)$$

where A_c indicates the diffraction peak areas of the amorphous region and A_a indicates the crystalline phase.

2.3.5 Colorimetric response of the films exposed to volatile ammonia

UV-Vis absorbance of the films was used to determine the sensitivity of the films to volatile ammonia (Kuswandi, Jayus, Restyana, et al., 2012). The colorimetric films (2 x 2 cm) were placed at 1 cm above the ammonia solution (0.8 M, 20 ml) for 16 minutes at 23 °C to measure changes in absorbance after exposure to ammonia vapor. Using a spectrophotometric instrument (Multiskan Sky, Thermo Scientific, Tokyo, Japan), the absorbance ratio of the films $\left(A_{605}/A_{530} \right)$ was measured minutely for 16 minutes. Placing (2 x 2 cm) film portions above the ammonia solution in beakers (25 ml) allowed for testing of the color response of films to various ammonia gas concentrations. Moreover, ammonium chloride (1 M) and sodium hydroxide were prepared to achieve the different concentrations of ammonia gas. Raoult's law was used to determine the concentration of gaseous ammonia by using the initial concentration of 20 ml ammonia solution and the partial vapor pressure at 23°C (Ma et al., 2018). In order to produce in situ ammonia gas concentrations equivalent to 5, 10, 20, 30, 60, 90, and 120 mg N/100 g at 23°C, a determined amount of stock solutions was injected into the beaker, and DI water was utilized as the reference solution (0 mg N/100 g). After the exposure to different concentrations of ammonia, the L* (lightness), a*(red to green), and b*(yellow to blue) values were obtained from the captured images with the help of the ImageJ program. The images were captured by the smartphone (LG, G6, Yeouido-dong, Seoul, South Korea) in a 3D printed holder. Finally, the ΔE^* values calculated with Eq. 4

$$[\Delta E]^* = [\,(\Delta L^*)^2 + (\Delta a^*)^2 + (\Delta b^*)^2\,]^{\,1/2} \qquad\qquad (4)$$

$$\Delta L^* = L_0^* - L^*,$$

$$\Delta a^* = a_0^* - a^* \quad \text{and}$$

$$\Delta b^* = b_0^* - b^* \quad \text{where } L_0^*, a_0^*, \text{ and } b_0^* \text{ were the reference samples.}$$

2.3.6   Chicken spoilage trails

Aseptically prepared 10 g of skinless chicken breast was added to the base of 5 cm-high polystyrene foam cups that had been exposed to UV light (254 nm for 15 minutes) for sterilization before the use. The colorimetric films were cut into small pieces (2x2 cm) and adhered to cellophane. The cellophane with the colorimetric sensor film was sealed 1 cm above the chicken samples. During the nine-day testing, the cups were kept at 4 °C. The smartphone (LG, G6, Yeouido-dong, Seoul, South Korea) was used to record the color change of the films. The captured images of the films were analyzed by calculating ΔE^* values as described above.

2.3.7   TVB-N measurements

The stomacher (Wisd, WES-400 model) was used to homogenize 10 g of skinless chicken breast in 100 ml sterile distilled water for 2 minutes. Next, the homogenate was centrifuged at 10000 rpm for 12 minutes, and the collected supernatant was combined with a volume-equal amount of magnesium oxide solution (1% w/v). The distillate from steam distillation was collected in a flask containing 25 ml of boric acid (20 g/l) and a few drops of methyl red/bromocrosol green indicator (Yildiz et al., 2021). The final mixture was titrated with 0.01M HCl until the blue color turned pink. The TVB-N was calculated with Eq. 5

$$\text{TVB-N (mg/100 g sample)} = \frac{(V_1 - V_0)0.14 \times 1 \times 100}{M} \tag{5}$$

where V_1 (ml) was the volume of 0.01M HCl solution for the sample, V_0 (ml) was the volume of 0.01 M HCl solution for blank, and M (g) was the weight of the sample.

2.3.8 Microbial analysis

Stomacher (Wisd, WES-400 model) was used to homogenize 10 g of skinless chicken breast sample with 100 mL of sterile peptone water for 2 minutes. Several decimal dilutions were carried out following the suggested microbiological methods to determine the total number of viable aerobic bacteria in the samples. Briefly, 1 ml of these dilutions were poured on Plate Count Agars. These inoculated Petri dishes were incubated aerobically at 30 °C for 48 hours (Rukchon et al., 2014). Colony-forming units (CFU) were recorded and expressed as log cfu/g.

2.3.9 Statistical analysis

All experiments were performed in triplicate. Statistical analysis of data was performed with software (OriginPro), and Tukey's posthoc test was used to detect statistical differences (p<0.05).

CHAPTER 3

RESULTS AND DISCUSSION

3.1   RCA optical characterization

Food packages evolve in response to meet consumer demand. The colorimetric films monitor the real-time status of the packaged products. In that sense, RCA doped colorimetric films can be used to detect food spoilage visually. RCA offers a dynamic and reversible color change in a wide spectrum upon protonation/deprotonation of hydroxyl groups on the phenolic rings of anthocyanins. Particularly for protein-rich food, the onset of spoilage leads to the release of total volatile basic amines. When RCA is exposed to these amine gases, the color of RCA changes dynamically. This visible color change can inform the consumers about the real-time condition of the food in the package. The color transition of RCA solutions was shown in the inset image of Fig 3.1. over the pH range from 1 to 12. The RCA solutions were reddish-pink at pH levels under 5, and at pH 6-7, the color gradually changed to purple. The color turned different hues of green at pH levels between 8 and 11 and turned yellow at pH 12. The colorimetric characteristics of RCA solutions matched those of red cabbage extracts reported in the literature (Abedi-Firoozjah et al., 2022). The maximum absorption peak was measured at 520 nm for pH values between 1 to 5, and the intensity of this peak gradually decreased from pH 1 to pH 7 as a result of bathochromic and hypochromic effects due to the proton transfer reaction of flavylium cation. The maximum absorption peak at 610 nm increased moderately as the hyperchromic effect predominated from pH 7 to pH 10, as shown in UV-Vis spectra of RCA in Fig 3.1. The spectrum of RCA solutions was in line with the previous literature studies (Liang et al., 2019).
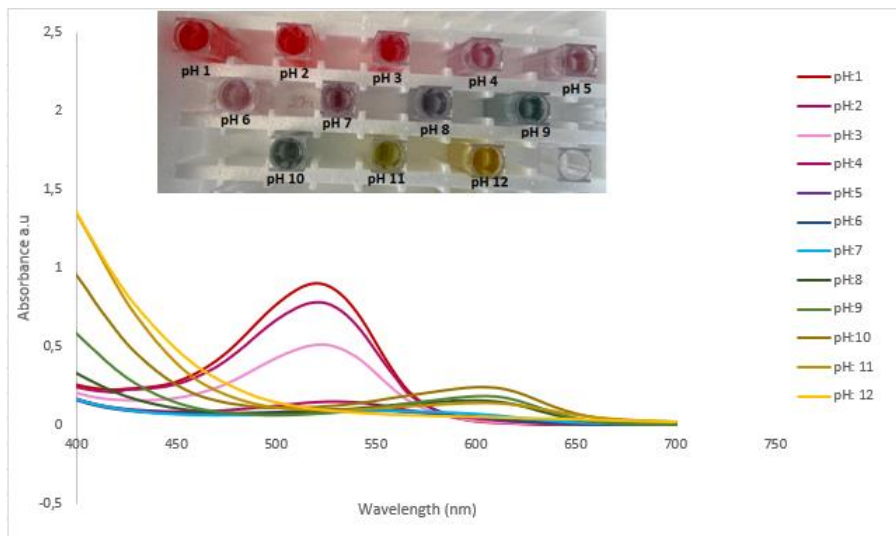
Figure 3. 1. UV-Visible absorption spectra and color change with pH variation of RCA.

3.2 Optical and physical characterization of C-dots

The C-dots showed a maximum absorption peak at around 360 nm (Fig. 3.2), which was attributed to the π-π* transition of the sp^2 domain and η- π* transitions of C=O and other functional groups that contain oxygen (Amjad et al., 2019).
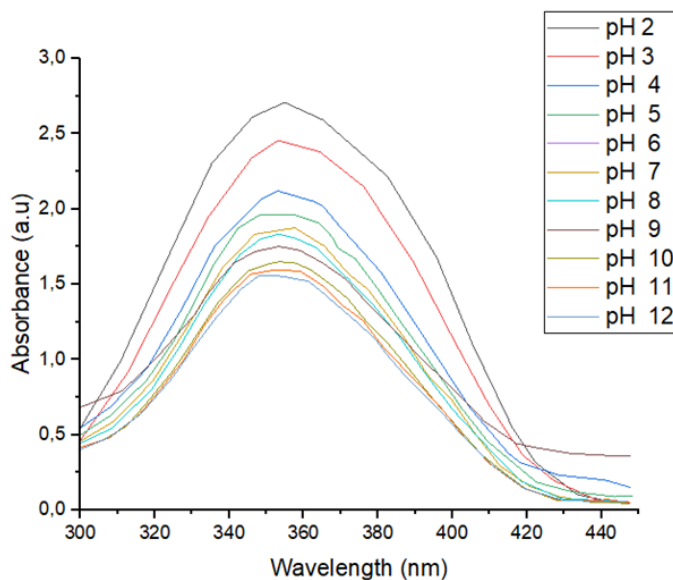

Figure 3. 2 UV-Visible absorption spectra of C-dots at pH 2 to pH 12

The high-resolution transmission electron microscope (HRTEM) was used to investigate the size and morphology of C-dots (Fig 3.3a). The synthesized C-dots had a spherical shape and were uniformly distributed in the solution, as demonstrated by the HRTEM image. The XRD analysis was performed to investigate the atomic arrangement and crystallinity of C-dots. The XRD analysis displayed a diffraction peak at about 21° ascribed to an effective carbonization process (Fig 3.3b) (Liu et al., 2017). In other words, the partial carbonization and amorphous character of C-dots can cause the observed broad diffraction peak obtained from XRD analysis (Ludmerczki et al., 2019).
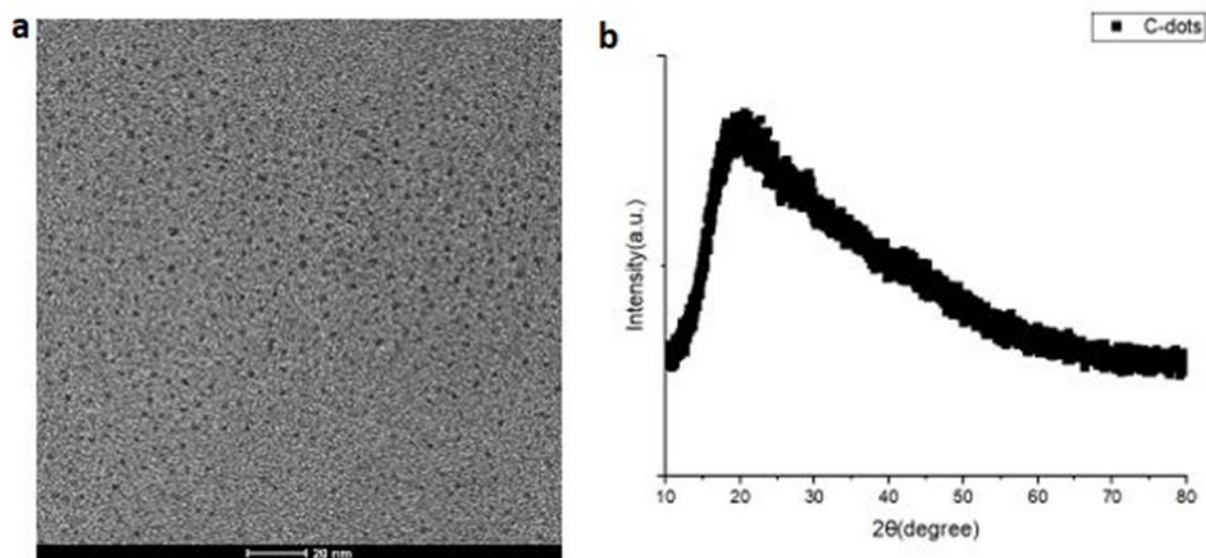
Figure 3. 3. TEM image of C-dots (a) and X-Ray Diffraction pattern of C-dots (b)

The FTIR spectrum provides information regarding interactions and alterations of chemical bonds on C-dots (Fig. 3.4). The characteristic O-H stretching vibration peaks of the carboxylic group were observed at 3226 cm^{-1} and 1136 cm^{-1}. The peak at 2887 cm^{-1} was ascribed to the C-H vibration while peaks at 1592 cm^{-1} and 1415 cm^{-1} were associated with asymmetric and symmetric stretching of the COO$^-$ groups (Xu et al., 2015). Peak at 1726 cm^{-1} was attributed to C=O stretching of the carboxylic group of C-dots. Consequently, it was associated with the surface carboxylic functional group (Dhenadhayalan et al., 2016). The presence of the

carboxylic group proves that successfully synthesized C-dots here can act as a chemical crosslinker using carboxylic groups as hypothesized.
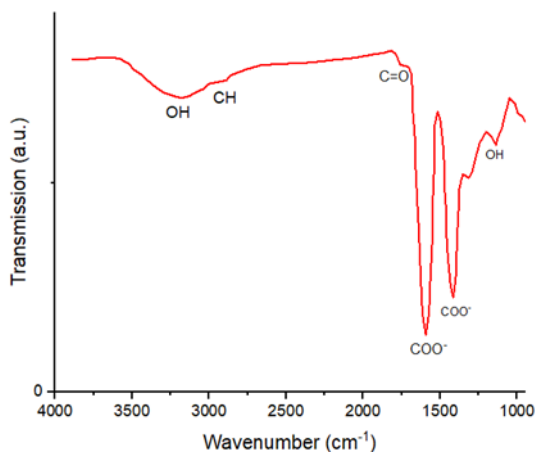
Figure 3. 4. FTIR spectra of C-dots

3.3 Surface functional groups analysis

The FTIR spectrums of RCA and fish gelatin films are given in Fig. 3.5. The hydroxyl stretching broad peak was observed at 3262 cm^{-1} and the peak at 2921 cm^{-1} was ascribed to the CH stretching vibration due to the aromatic ring in the RCA structure (Gokilamani et al., 2013). The flavylium cation of anthocyanins at the B ring might lead to the observed stretching vibration peak at 2362 cm^{-1} while the C=C stretching from the benzopyran aromatic ring caused an observed peak at 1598 cm^{-1}. Moreover, the peak at 1400 cm^{-1} was associated with the angular deformation of phenols and the peak that appeared at 1033 cm^{-1} was attributed to the aromatic ring of the flavonoid compound (Ramamoorthy et al., 2016; Pereira et al., 2015). The characteristic bands for N-H stretching vibration of Amide A and the free or bounded hydroxyl groups over 3000 cm^{-1} and for C-H stretching vibration of Amide B around 2900 cm^{-1} were observed in all fish gelatin films. In addition, all fish gelatin films had peaks around 1646 cm^{-1}, 1567 cm^{-1} 1265 cm^{-1}. These peaks showed the C=O and C-N stretching of Amide I, N-H bending, and C-N stretching of Amide II, as well as the vibration of N-H and C-N groups of Amide III,

32

respectively (Li et al., 2016). As shown in Fig. 3.5b, all films had matching spectra. However, the addition of C-dots affected the intensity of Amide I and Amide II. The effect of C-dots addition was more pronounced with increasing the C-dot concentration in the film matrix. For example, for the FG-UV-100 samples, the decrease in intensity of the Amide I band was more observable than in other samples. Furthermore, the band at 1067 cm^{-1} was related to hydrogen bonding between the C-dots, glycerol, and FG. On the other hand, the band at 1428 cm^{-1} was attributed to the hydroxyl bending of carboxylic acid (Li et al., 2016; Bhattacharyya et al., 2020). Further, these peaks were broader and sharper with the addition of 100 mg/l of C-dots. The results also matched the literature where citric acid and C-dots were added into gelatin-based films as crosslinkers (Uranga et al., 2016; Bhattacharyya et al., 2020). As shown in Fig. 3.4 and Fig. 3.5b, the peak ascribed to C=O stretching of the carboxylic group of C-dots at 1726 cm^{-1} was not observed in FG films which might be attributed to crosslinking between the carboxylic group of C-dots and the amine groups from FG. Theoretically, imide and amide bond formation might occur in the presence of the carboxylic group and amine group in the matrix (Uranga et al., 2016). The FTIR spectra showed no peak at 1770 cm^{-1}, the presence of which is an indicator of imide bond formation On the other hand, an amide I bond peak was observed at 1646 cm^{-1}. As a result, the main crosslinking process in this study was thought to be the formation of amide bonds. Similar results were observed in the literature (Bhattacharyya et al., 2020; Uranga et al., 2016). Moreover, in this study, the precursor solution was prepared under basic conditions to facilitate the crosslinking reaction between the carboxylic group and amine group, which is anticipated to cause nucleophilic substitution and subsequently result in the formation of amide bonds (Bhattacharyya et al., 2020). Under the basic condition, the carboxylic acid group from C-dots deprotonated and formed carboxylates. The amine group of FG attacks the carboxylates and forms stable amide bonds (Reddy et al., 2009; Uranga et al., 2016).
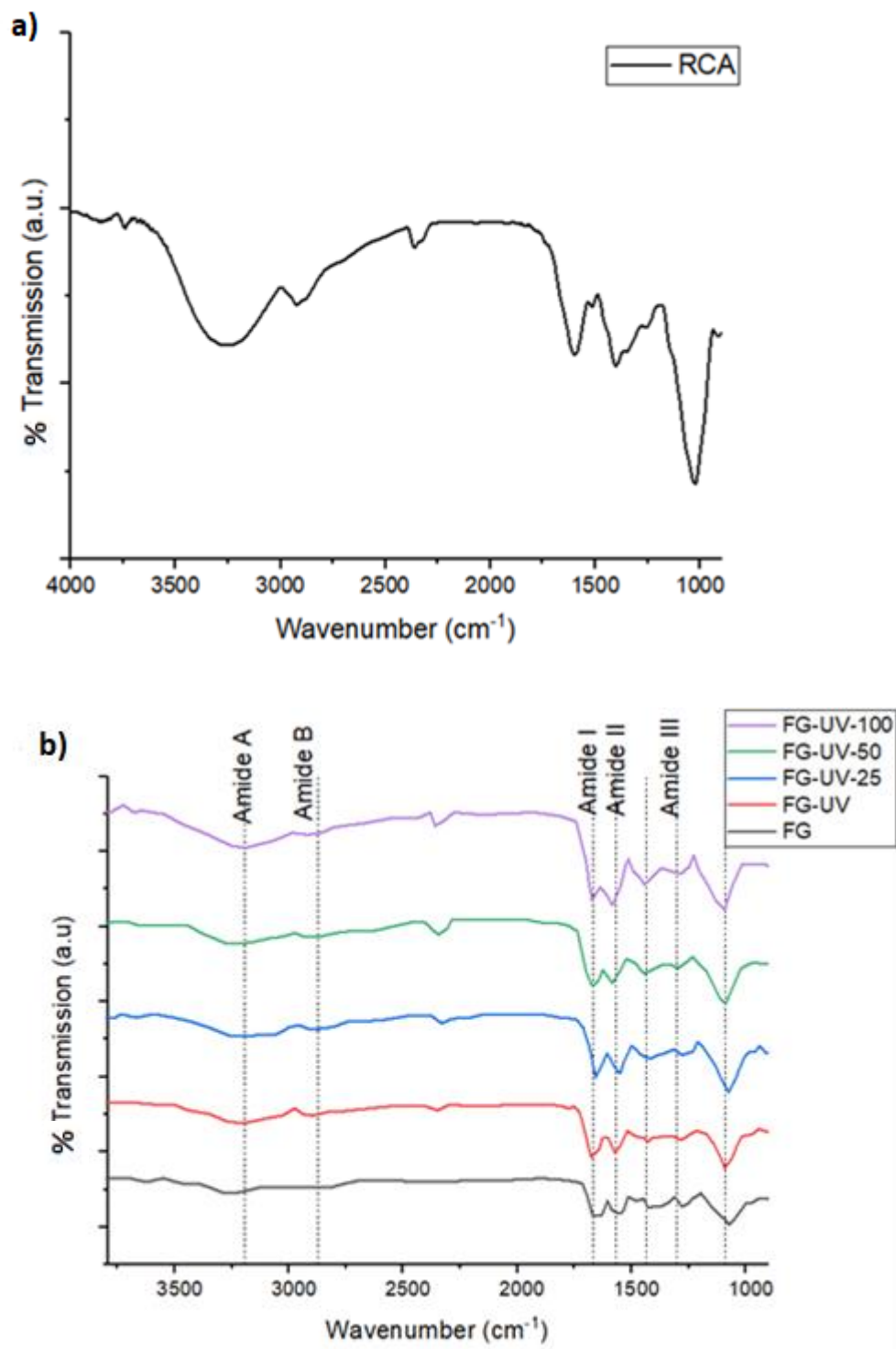
Figure 3. 5. FTIR spectra of all RCA (a), and FG films (b)

3.4   FG films structural analysis

The X-ray diffraction method was used to investigate the crystallinity of FG films, as described in section 2.2.4. Fig. 3.6 illustrates the XRD diffraction patterns of these samples. The diffraction bands of FG films doped with C-dots indicated that there were not any distinct peaks due to C-dots addition. It might be due to the low content of C-dots in films or well-dispersed C-dots in the film matrix. The XRD patterns had peaks at $2\theta = 7.5°$ and a broader one at $2\theta = 20°$. The peak at $2\theta = 7.5°$ was attributed to the triple helix crystalline structure of the films, while the peak at $2\theta = 20°$ was ascribed to peptide bonds (Sajkiewicz & Kolbuk, 2014), (Nor Adilah et al., 2021). Both of these peaks demonstrated the partially crystalline structure of the gelatin films (Coronado Jorge et al., 2015).

Figure 3. 6. X-Ray Diffraction pattern of FG films

UV exposure did not change the percent crystallinity of FG control films significantly as seen in Table 3.1. When the addition of C-dots to FG-UV films was

investigated, the results showed that incorporating C-dots decreased the crystallinity of the films (Table 2). FG films became more amorphous upon the addition of C-dots. The develop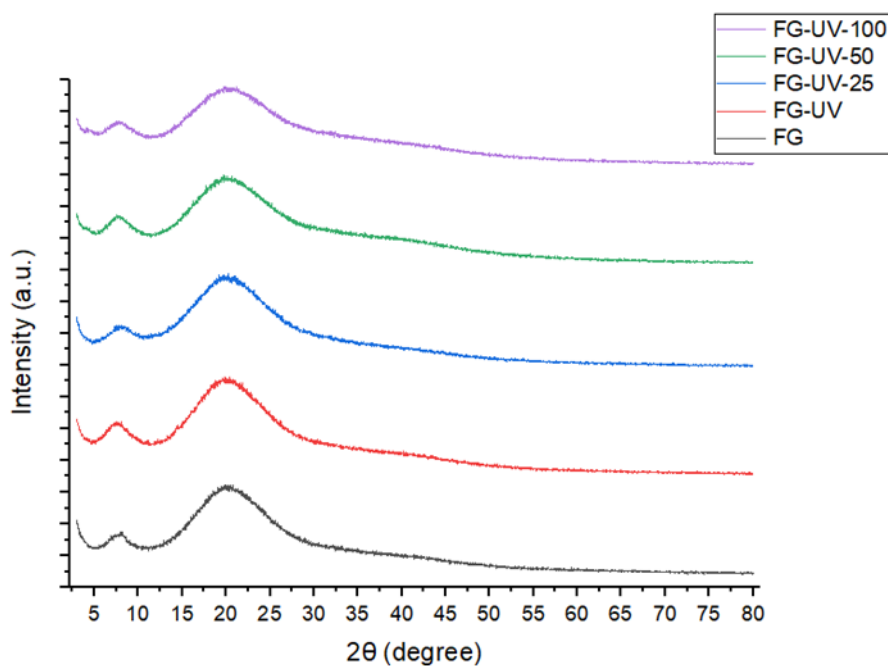ment of crosslinks between carboxylic and hydroxyl groups of C-dots and amine groups of gelatins may prevent gelatin from reassembling into its triple helix structure. Therefore, the intermolecular interaction between amino acid residues of gelatin reduces and causes crystallinity loss during the fabrication of the films (Etxabide et al., 2015; J. Guo et al., 2014). Similar results were reported in the literature. For instance, the study of gelatin composite films with graphene oxide suggested that the slower renaturation of the triple helix structure of gelatin could be the reason for the crystallinity loss of the gelatin composite films in the presence of oxygen-containing surface functional groups of graphene oxide (Wan et al., 2011).

Table 3. 1. The percent relative crystallinity of FG films *

FG film samples	Relative crystallinity (%)
FG	14.5 ± 0.3^{ab}
FG-UV	14.8 ± 0.1^{a}
FG-UV-25	14.1 ± 0.1^{abc}
FG-UV-50	13.7 ± 0.5^{bc}
FG-UV-100	13.1 ± 0.1^{c}

* Values are given as mean ± standard deviation. Means with the same superscripted letter not significantly different at $p < 0.05$

3.5 Thermal characterization

DSC is a practical method to determine the thermal stability of films (Becker & Locascio, 2002; Nilsuwan et al., 2018). The Tm (melting temperature) of blank FG films was 77.87 °C according to the DSC thermogram, while the Tm of UV-exposed FG films was increased to 86.13 °C (Fig. 3.7). UV irradiation produces free radicals that are mostly generated by the aromatic acyl residues of water and gelatin. These free radicals increase crosslinking density while decreasing gelatin chain segment mobility, which leads to an increase in Tm (Sharma et al., 2018). The Tm values increased to 87.24 °C, 90.68 °C, and 93.78 °C when the C-dots concentration increased as illustrated for FG-UV-25, FG-UV-50, and FG-UV-100 in Fig. 3.7,

respectively. As mentioned before, C-dots can be used as a chemical crosslinker during the fabrication of FG films. Therefore, the addition of C-dots to FG films was expected to increase the crosslinking density and, thereby, the Tm of CD-doped FG films. Similar results were observed in the literature. Masutani et al., (2014) reported that Tm values of gelatin films increased upon crosslinking with glucose. These findings suggested an increase in Tm of FG films with the addition of C-dots. It might be explained by amide and hydrogen bond formation between C-dots and fish gelatin, which limits the chain mobility of gelatin. Consequently, the DSC findings verify the findings of the XRD analysis discussed in the previous section.
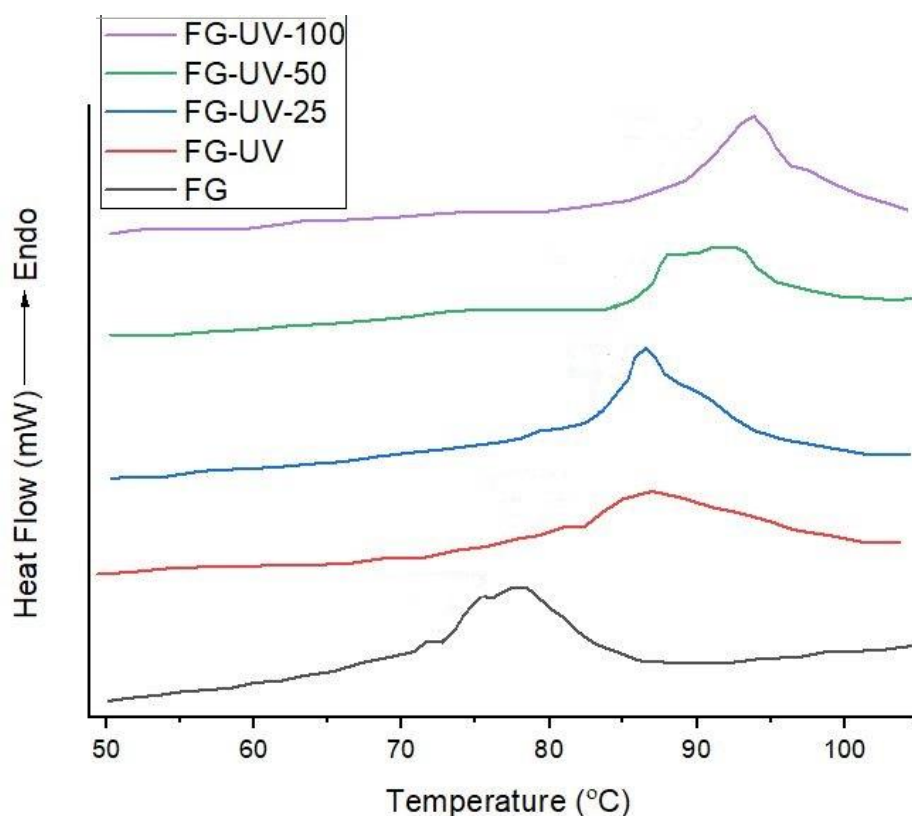

Figure 3. 7. DSC thermogram of Fg films

3.6   Water solubility, barrier, and mechanical analysis of FG films

Water solubility (WS) defines the water resistance of the films. As illustrated in Table 3.2, untreated FG control films showed the highest WS of 82%. Similar WS

value for cold-water fish gelatin values was observed in the literature (Jeya Shakila et al., 2012). Exposure to UV irradiation even before the addition of C-dots resulted in a dramatic reduction of WS values of the films. This drastic reduction in WS can be explained by an increase in the crosslinking density of FG films. Radicals produced at the aromatic amino acid residues of gelatin might induce the crosslinking of gelatin under UV irradiation (Bhat & Karim, 2014). In addition to UV irradiation-induced physical crosslinking, the introduction of chemical crosslinking with the surface functional groups of C-dots decreased the WS considerably, as expected.

The WS values of FG films exposed to UV and doped with different C-dots concentrations (25 mg/l, 50 mg/l, and 100 mg/l) were 56%, 49%, and 38%, respectively. The lowest WS was observed in the FG films with the highest C-dots concentration. This result is in line with the previous literature studies, where a similar effect on the WS of FG films was observed upon adding chemical crosslinkers such as sugar (Hazaveh et al., 2015; Kchaou et al., 2018). Overall, the presence of both physical (UV irradiation) and chemical (C-dots) crosslinkers boosts the cross-linking in the matrix by increasing the intermolecular interactions and, in turn leading to a drastic reduction in WS values of FG films

Table 3. 2. Water solubility of FG films*

FG film samples	WS (%)
FG	82.3 ± 3.37^a
FG-UV	63.5 ± 3.39^b
FG-UV-25	56.3 ± 1.59^{bc}
FG-UV-50	49.8 ± 2.80^c
FG-UV-100	38.8 ± 2.18^d

* Values are given as mean ± standard deviation. Means with the same superscripted letter not significantly different at $p < 0.05$

Tensile strength (TS) and elongation at break (EAB) values are shown in Table 3.3. One of the significant properties in defining the mechanical properties of food packaging films is TS. After UV irradiation, the TS of films significantly increased.

The previous studies also showed that UV irradiation treatment improved the TS of FG films (Bhat & Karim, 2014; Otoni et al., 2012). Further, the addition of C-dots also affected the TS of FG films. As discussed before, the incorporation of C-dots increased the intermolecular interaction by the amide and hydrogen bond formation between the surface functional groups of C-dots and FG. This result was also seen in the surface analysis of ATR-FTIR. It resulted in an improvement of TS when compared to the control FG films. The acquired results were similar to the previous studies, which investigated the effects of C-dots on TS of soy protein isolate and gelatin/carrageenan composite films (Li et al., 2016; Roy et al., 2021).

The change in EAB was used to determine the effect of physical and chemical crosslinking agents on the flexibility of the films. The UV treatment results showed the opposite trend with TS results. A similar trend between TS and EAB has already been documented in the literature (Dainelli et al., 2008). Furthermore, EAB values of FG films treated with C-dots and UV irradiation indicated significant differences from those not treated with UV irradiation. On the other hand, there was not a significant difference when EAB values of C-dots treated films were compared. However, there was a decreasing tendency in EAB values of FG-UV films when C-dots concentration increased. While increasing the C-dots concentration in the film matrix, the C-dots and FG interaction might be increased since the restriction in the matrix motion could occur. Some studies on C-dots incorporated soy protein isolate film showed a similar trend of mechanical properties upon the addition of C-dots (Li et al., 2016; Rani et al., 2020). In conclusion, the mechanical properties of FG films improved after C-dots addition and UV exposure. The strong FG and C-dots interactions might explain this improvement as a result of amide and hydrogen bond formation under UV irradiation.

Table 3. 3 Mechanical properties of FG films*

FG film samples	TS(MPa)	EAB (%)
FG	22.6 ± 0.60^a	223.2 ± 20.2^a
FG-UV	30.7 ± 0.57^b	117.8 ± 4.21^b
FG-UV-25	34.5 ± 1.12^c	136.8 ± 5.76^b
FG-UV-50	34.9 ± 1.47^c	124.2 ± 8.11^b
FG-UV-100	36.9 ± 0.42^c	120.7 ± 1.87^b

* Values are given as mean ± standard deviation. Means with the same superscripted letter in the same column not significantly different at $p < 0.05$

Water vapor permeability (WVP) is described as the water vapor passage ability of a material. It is an important parameter for the packaging industry to maintain product quality. As a consequence, a low WVP value is essential for the packaging films to restrict the water vapor transition and maintain the package atmosphere. During the WVP measurements, the characteristic thickness of the hydrophilic film should be taken into account carefully as there is a positive correlation between the film thickness and the WVP (McHUGH et al., 1993). In this study, the thickness of FG films did not show a significant difference when exposed to UV irradiation and/or with the addition of C-dots (Table 3.4) (p<0.05). Although there was a decreasing tendency in the WVP among control samples of FG films (Table 3.4), this decrease was not statistically significant. Correspondingly, an insignificant decrease in UV-treated protein films was also illustrated in the literature (Rhim et al., 1999). When the effects of C-dots concentration on WVP properties of FG-UV films were examined, the results showed that WVP dramatically decreased as C-dots concentration increased in the film matrix compared to untreated FG films (p<0.05). The WVP of highly hydrophilic protein-based films could be reduced with extensive cross-linking. The creation of the H-bonds and covalent conjugation between C-dots and FG might be attributed to this decrease. The accessibility of the hydrophilic groups of gelatins might be reduced with the H-bond formation and covalent conjugation since extensive crosslinking increases the complexity of the diffusion

pathway. Consequently, water vapor penetration was reduced (J.-E. Lee & Kim, 2010; Li et al., 2016).

Table 3. 4. Water vapor permeability and thickness of FG films*

FG film samples	Thickness(mm)	WVP $*10^{-10}$ (g m^{-1} s^{-1} Pa^{-1})
FG	0.19 ± 0.01^a	7.12 ± 1.10^a
FG-UV	0.17 ± 0.02^a	5.32 ± 0.21^{ab}
FG-UV-25	0.16 ± 0.01^a	4.57 ± 0.30^{bc}
FG-UV-50	0.17 ± 0.01^a	4.53 ± 0.04^{bc}
FG-UV-100	0.20 ± 0.01^a	2.97 ± 0.07^c

* Values are given as mean ± standard deviation. Means with the same superscripted letter in the same column not significantly different at $p < 0.05$

3.7 Microstructural characterization of FG films

FESEM was used to examine the cross-sectional morphology of the FG films. The untreated FG control films displayed a generally smooth and dense structure. This structure could be explained by a low degree of intermolecular interaction. Mechanical properties of tested FG films also supported this explanation, where the lowest TS was observed in untreated FG films. UV exposure did not cause a significant change in the morphology of control films. On the other hand, the C-dot addition caused the crack and rough cross-sectional view (Fig. 3.8). This morphological alteration became more apparent when C-dots content in the FG films increased (Bhattacharyya et al., 2020). The crystalline phase transition of the FG matrix, as discussed in section 3.4, and the increased mechanical characteristics of FG films upon C-dot addition both support this visual evidence. As illustrated in Fig. 3.8, the wavy and uneven cross sections could be concrete proof of improved crosslinking after adding C-dots into the film matrix.
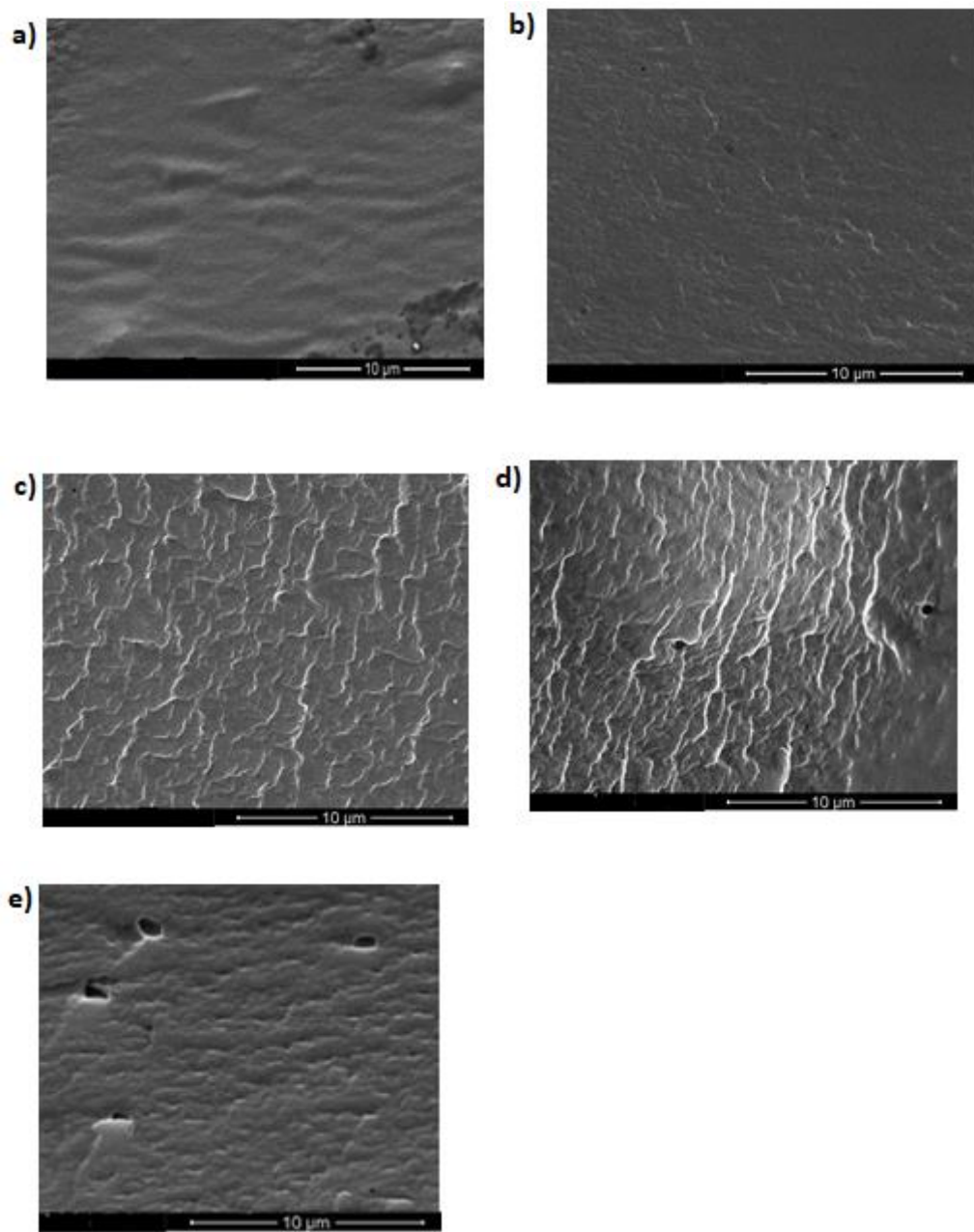
Figure 3. 8. FESEM images of FG films (scale bar 10 μm) a) FG, b) FG-UV,
c) FG-UV-25, d) FG-UV-50, e) FG-UV-100

3.8   Colorimetric response of FG films exposed to ammonia vapor

Volatile basic amines, such as ammonia, tri-, and dimethylamine, are released during bacterial and enzymatic activities of protein-rich products (J. Zhang et al., 2019; Moradi et al., 2019). Ammonia has the lowest boiling point among the most commonly released TVB-N compounds, which are ammonia, trimethylamine, and dimethylamine, during spoilage. Therefore, ammonia was selected as the representative of TVB-N compounds, which are responsible for the sensorial detection of deterioration of foods (Ezati et al., 2019). Ammonia causes a color shift in the films by interacting with hydroxyl groups of anthocyanins (Moradi et al., 2019; Zhai et al., 2017). The colorimetric response of films to gaseous ammonia was investigated in this study. Following this purpose, the FG films were subjected to ammonia gas produced from 0.8 M aqueous ammonia solution for 16 min at 23°C. Initially, all films had the highest absorption peak at 530 nm, which was red-shifted from the peak of RCA solution at 520 nm. Similar results were also reported in the literature. Absorption spectra of the starch-polyvinyl alcohol-based film containing anthocyanins of Roselle (*Hibiseus sabdariffa L.*) showed a red shift when anthocyanins were doped to starch and polyvinyl alcohol films (Zhai et al., 2017). The absorbance peak of FG films at 530 nm decreased with the release of ammonia gas over time while a new peak appeared at 605 nm, and the peak intensity was progressively increased. The absorbance ratio (A605 / A530) of films shows how intensely the green color hue was compared to red (Choi et al., 2017). The ratio was increased with time, as shown in Fig. 3.9. The slope is related to the rate of color change; therefore, a higher slope indicates a larger variation in color. In another word, it shows how quickly the color changed from red to green (Zhai et al., 2017). The control samples exhibited the lowest rate, and the rate increased with increasing C-dot concentration in the films. As a result, the film with the highest C-dot concentration showed the most rapid color change. Thus, among the tested films, FG-UV-100 films were the most sensitive to ammonia and TVB-N compounds.

a)

b)
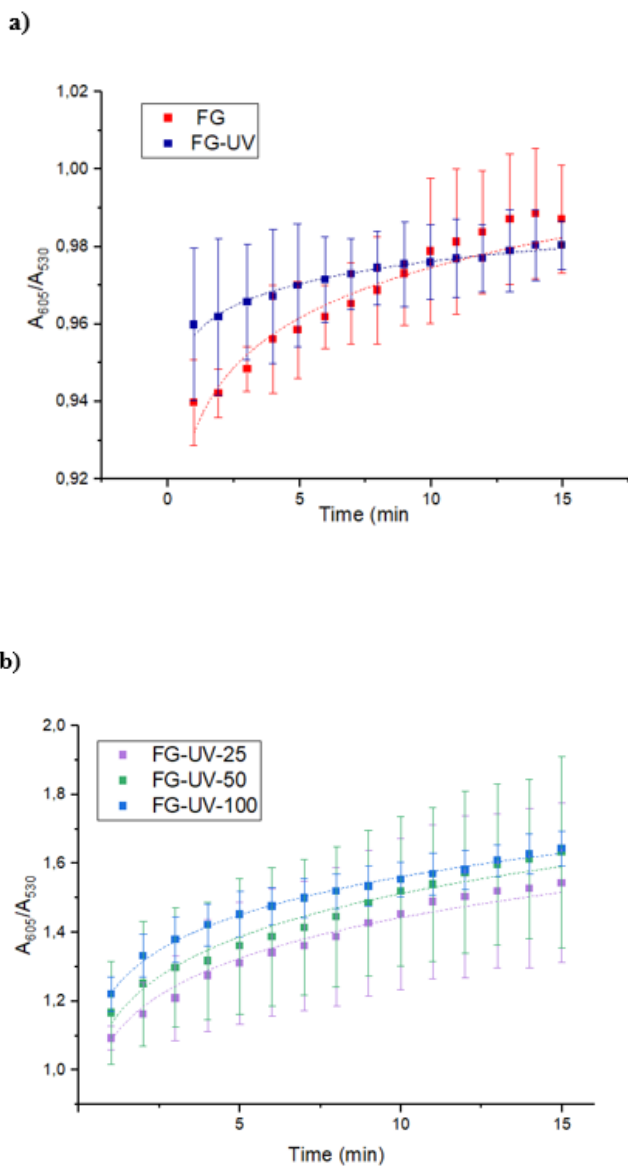
Figure 3. 9. UV-Visible absorption changes of FG, FG-UV, FG-UV-25, FG-UV-50, and FG-UV-100 films when exposed to the 0.8 M ammonia vapor for 16 min

C-dots are affected by the pH change, the bright yellow appearance was observed in acidic conditions, and the color changed progressively from yellowish to orange, as shown in Fig 3.10. Similarly, the effect of pH on the color change of C-dots was reported earlier and has been linked to the electronic transition shift between the π-

π* and η- π* in nanodomains during refilling or discharging their valance bands (Chen & Yan, 2011; Jia et al., 2012). This supported that the color sensitivity according to ammonia vapor was increased by increasing the C-dots concentration on films discussed before. As a result, the most sensitive sample was decided to be FG-UV-100 films against ammonia in this study.
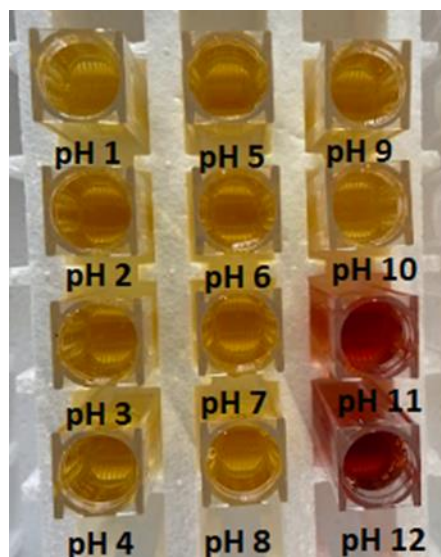
Figure 3. 10. Visual color variation of C-dots in response to different pH values in the range of 1 to 120

Among the tested films, FG-UV-100 films were selected with superior properties to examine the potential use in intelligent packaging applications. For this purpose, the change in a* and ΔE values were evaluated upon exposure to different ammonia concentrations (Fig. 3.11). The color changes and ammonia gas concentration were tabulated in Table 3.5. The color changed from red to green, with the ammonia concentration increasing from 0 to 120 mg/ 100g. A significant change in ΔE values was observed starting with the ammonia concentration of 5 mg / 100 g ($p<0.05$). The a* value indicates the color intensity transition from green to red from -a* to a* in the CIEL*a*b* system. There was a negative correlation between a* and ΔE values (r= -0.99). In other words, this value decreased with increasing the ammonia concentration. Similarly, the ΔE value that defines the color difference increased with increasing the ammonia concentration significantly ($p<0.05$).
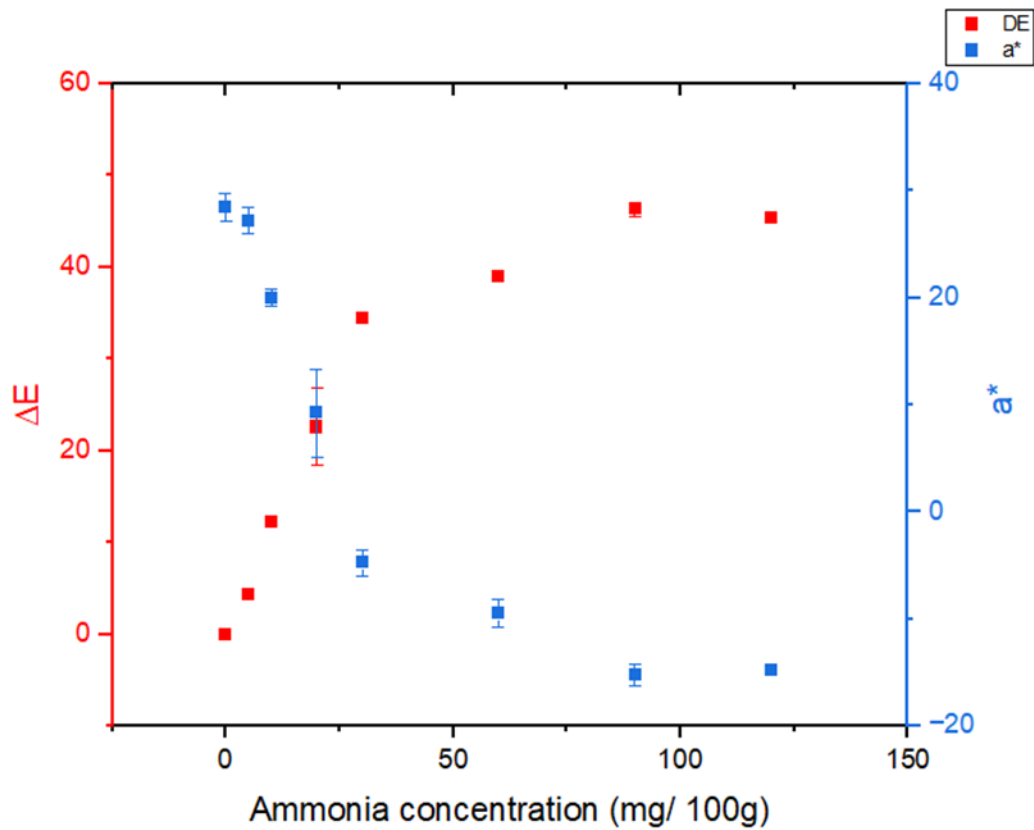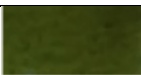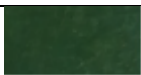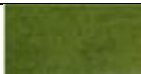
Figure 3. 11. ΔE and a* change of FG-UV-100 film exposed to varying concentrations of ammonia

The human eye can differentiate the color difference when the value of ΔE value exceeds 5 (Naghdi et al., 2021). In this study, ΔE values of the films exceeded this critical level for all ammonia concentrations tested (Fig. 3.11). The findings above demonstrated the remarkable detection performance of FG-UV-100 films in response to the varying concentrations of volatile ammonia. Therefore, FG-UV-100 films were tested with a real food sample.

Table 3. 5. The color change of the FG-UV-100 film exposed to varying concentrations of ammonia gas

C$_{ammonia\ gas}$	Film images exposed to ammonia gas
0 mg/ 100g	
5 mg/ 100g	
10 mg/ 100g	
20 mg/ 100g	
30 mg/ 100g	
60 mg/ 100g	
90 mg/ 100g	
120 mg/ 100g	

3.9 Application of film in chicken spoilage trials

Total viable count (TVC) is a simple and frequently used microbiological technique that provides information about microbial quality by counting the viable number of microorganisms in the food sample. TVC regulates the condition of products from processing line to distribution. Thus, the TVC level was monitored to examine the microbial quality of skinless chicken samples during the storage at 4°C. TVC values of chicken samples considerably increased during 9 days of storage as shown in Fig. 3.12.

According to European Law (EC Regulation 1441/2007, 2007) and the Turkish Standards (TS 24019:2014), the upper limit of TVC for raw chicken breast is 6.7 logcfu/g. After 7 days, the permitted level of total aerobic bacteria was reached and

surpassed. This result complies well with the study on broiler chicken freshness monitoring by Kuswandi et al. (2014).
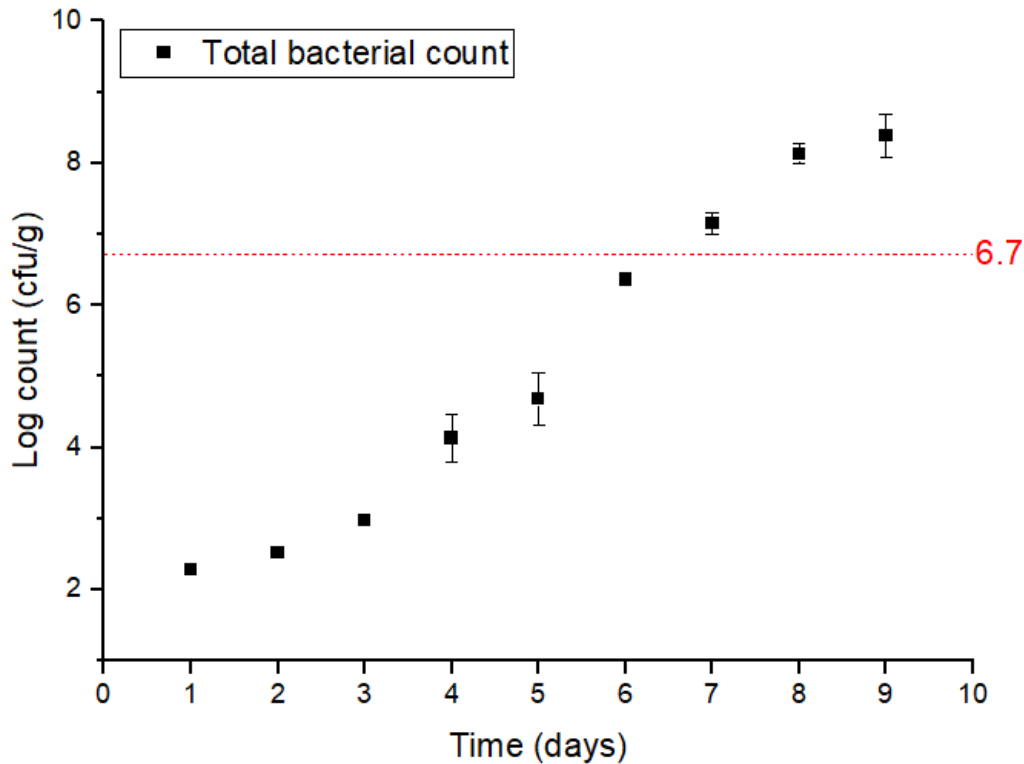
Figure 3. 12. Total viable count during 9 days of storage at 4°C of chicken breast

TVB-N compounds are by-products of the destructive actions of microorganisms and metabolic processes. The release of TVB-N compounds during spoilage is responsible for the off-flavor formation in protein-rich food. Thus, the level of TVB-N is one of the most significant freshness indicators. Therefore, in this study, the TVB-N level served as the real-time indicator to monitor the freshness of the chicken sample with FG-UV-100 films. When the chicken breast spoilage was initiated, it was expected to give a colorimetric response to TVB-N of FG-UV-100 films. The a* and ΔE values were measured during 9 days of storage at 4 °C. The color transition was shown in Table 3.6. The a* and ΔE values were not indicated a significant difference during the first five days; correspondingly, the color difference of the films was not significant during the same period.
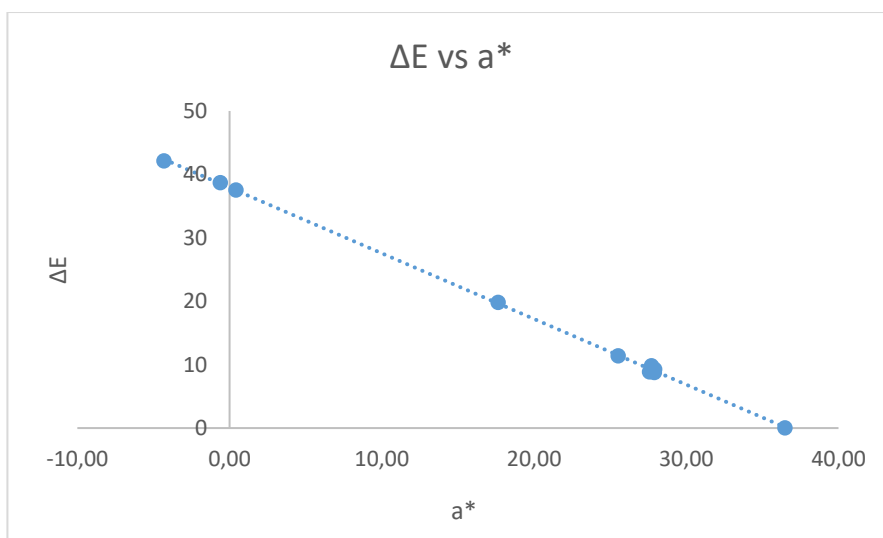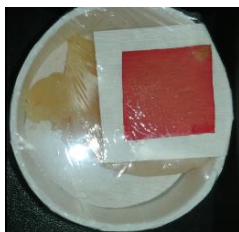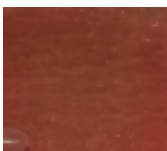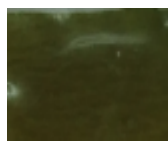
Figure 3. 13. The changes in ΔE and a* values of FG-UV-100 film during the storage period at 4°C

The Turkish Standard has established the TVB-N threshold limit for poultry carcasses at 30 mg N/ 100g (TS2409:2014). In the first 6 days, TVB-N levels were below this threshold limit. On the 7th day, the TVB-N level reached 30.2 ± 1.98 mg N/ 100 g. Therefore, on the 7th day, the chicken samples were at the onset of spoilage. This result was supported by the color transition of FG-UV-100 films after 6 days. The color of the film was changed to green from pinkish-red at the 7th day. Correspondingly, the a* value was significantly decreased, and ΔE value was increased during this period (Fig. 3.13). The ΔE and a* values of films showed a negative correlation (r= -0.99).

Both the TVB-N level and the microbial load increased gradually during the 9-day storage at 4 °C (Table 3.6 & Fig. 3.12). After 7 days of storage, the threshold limit of the TVB-N value and the maximum allowable level of TVC were both attained. This result is consistent with that of Kuswandi et al. (2014) study, which examined the TVB-N level of chicken stored at 4 °C and indicated the level was exceeded after 7 days. Consequently, the FG-UV-100 film displayed a significant color change (also a* and ΔE values) parallel to the TVB-N and TVC change during 9-day storage (Table 3.6).

Table 3. 6. The TVB-N change of the skinless chicken breast and the color response of FG-UV-100 film during storage at 4°C*

Storage time (day)	0	1	2	3	4
TVB-N (mg N /100g)		11.3 ± 0.40^a	12.14 ± 0.26^a	12.96 ± 0.66^a	14.5 ± 0.13^a
Color response					
Storage time (day)	5	6	7	8	9
TVB-N (mg N /100g)	16.6 ± 0.98^a	21.9 ± 2.31^{ab}	30.2 ± 1.98^{bc}	41.62 ± 3.96^{cd}	44.14 ± 6.99^d
Color response					

* Values are given as mean ± standard deviation. Means with the same superscripted letter in the same row not significantly different at $p < 0.05$

CHAPTER 4

CONCLUSION AND RECOMMENDATIONS

In this study, the colorimetric FG film was fabricated with RCA extract, C-dots, and FG to monitor food spoilage using color transition. In general, FG-based films show poor mechanical properties; therefore, the crosslinkers, C-dots as chemical and UV irradiation as physical, were used to enhance the physicochemical properties of FG films in this study. The effect of UV irradiation exposure and C-dots on FG films were examined in terms of mechanical, water solubility, barrier, thermal, and structural properties. The FTIR spectra of fabricated colorimetric films demonstrated that C-dots were successfully integrated into the fish gelatin matrix through the formation of amide bonds. Furthermore, the crystallinity of the FG films was decreased with the increased crosslinking by the interaction between C-dots and amino acid residues. Therefore, the mechanical, barrier, solubility, and thermal properties of films were improved upon the addition of C-dots under UV irradiation. In addition, the color response of FG films against the different concentrations of ammonia vapor was investigated to test their applicability as an intelligent packaging label. The film with the highest C-dots concentration (FG-UV-100) was the most sensitive film in response to ammonia vapor. During real food trials, the color response of FG-UV-100 films showed a positive correlation (r=0.91) with microbial growth and TVB-N release in protein-rich skinless chicken breast samples (p=0.0006<0.05). Thus, the film can potentially be used in real-time monitoring of spoilage.

For future studies, C-dots concentration may be increased in fish gelatin-based films. The red cabbage extract may be obtained with another solvent to increase the extraction yield, such as ethanol. Instead of red cabbage, different sources can be used to extract anthocyanins. A different source may be used to obtain C-dots other than citric acid.

REFERENCES

Abedi-Firoozjah, R., Yousefi, S., Heydari, M., Seyedfatehi, F., Jafarzadeh, S., Mohammadi, R., Rouhi, M., & Garavand, F. (2022). Application of Red Cabbage Anthocyanins as pH-Sensitive Pigments in Smart Food Packaging and Sensors. *Polymers*, *14*(8). https://doi.org/10.3390/polym14081629

Alizadeh-Sani, M., Mohammadian, E., Rhim, J. W., & Jafari, S. M. (2020). pH-sensitive (halochromic) smart packaging films based on natural food colorants for the monitoring of food quality and safety. *Trends in Food Science and Technology*, *105*(January), 93–144. https://doi.org/10.1016/j.tifs.2020.08.014

Amjad, M., Iqbal, M., Faisal, A., Junjua, A. M., Hussain, I., Hussain, S. Z., Ghramh, H. A., Khan, K. A., & Janjua, H. A. (2019). *Nanoscale Advances bovine gelatin and PHM3 microalgae strain for*. 2924–2936. https://doi.org/10.1039/c9na00164f

Anastase-Ravion, S., Carreno, M. P., Blondin, C., Ravion, O., Champion, J., Chaubet, F., Haeffner-Cavaillon, N., & Letourneur, D. (2002). Synergistic effects of glucose and ultraviolet irradiation on the physical properties of collagen. *Journal of Biomedical Materials Research*, *60*(3), 384–391. https://doi.org/10.1002/jbm.10111

Averous, L., & Boquillon, N. (2004). Biocomposites based on plasticized starch: Thermal and mechanical behaviours. *Carbohydrate Polymers*, *56*(2), 111–122. https://doi.org/10.1016/j.carbpol.2003.11.015

Azeredo, H. M. C., & Correa, D. S. (2021). Smart choices: Mechanisms of intelligent food packaging. *Current Research in Food Science*, *4*, 932–936. https://doi.org/10.1016/j.crfs.2021.11.016

Azeredo, H. M. C. d. (2009). Nanocomposites for food packaging applications. *Food Research International*, *42*(9), 1240–1253. https://doi.org/10.1016/j.foodres.2009.03.019

Bae, H. J., Park, H. J., Hong, S. I., Byun, Y. J., Darby, D. O., Kimmel, R. M., & Whiteside, W. S. (2009). Effect of clay content, homogenization RPM, pH, and ultrasonication on mechanical and barrier properties of fish gelatin/montmorillonite nanocomposite films. *LWT - Food Science and Technology*, *42*(6), 1179–1186. https://doi.org/10.1016/j.lwt.2008.12.016

Becker, H., & Locascio, L. E. (2002). Polymer microfluidic devices. *Talanta*, *56*(2), 267–287. https://doi.org/10.1016/S0039-9140(01)00594-X

Bhargava, N., Sharanagat, V. S., Mor, R. S., & Kumar, K. (2020). Active and intelligent biodegradable packaging films using food and food waste-derived bioactive compounds: A review. *Trends in Food Science and Technology*, *105*(September), 385–401. https://doi.org/10.1016/j.tifs.2020.09.015

Bhat, R., & Karim, A. A. (2014). Towards producing novel fish gelatin films by combination treatments of ultraviolet radiation and sugars (ribose and lactose) as cross-linking agents. *Journal of Food Science and Technology*, *51*(7), 1326–1333. https://doi.org/10.1007/s13197-012-0652-9

Bhattacharyya, S. K., Dule, M., Paul, R., Dash, J., Anas, M., Mandal, T. K., Das, P., Das, N. C., & Banerjee, S. (2020). Carbon Dot Cross-Linked Gelatin Nanocomposite Hydrogel for pH-Sensing and pH-Responsive Drug Delivery. *ACS Biomaterials Science and Engineering*, *6*(10), 5662–5674. https://doi.org/10.1021/acsbiomaterials.0c00982

Boon, C. S., McClements, D. J., Weiss, J., & Decker, E. A. (2010). Factors influencing the chemical stability of carotenoids in foods. *Critical Reviews in Food Science and Nutrition*, *50*(6), 515–532.

https://doi.org/10.1080/10408390802565889

Brecht, J. K. (2019). Ethylene technology. *Postharvest Technology of Perishable Horticultural Commodities*, 481–497. https://doi.org/10.1016/B978-0-12-813276-0.00014-6

Calva-Estrada, S. J., Jiménez-Fernández, M., & Lugo-Cervantes, E. (2022). Betalains and their applications in food: The current state of processing, stability and future opportunities in the industry. *Food Chemistry: Molecular Sciences*, *4*(November 2020). https://doi.org/10.1016/j.fochms.2022.100089

Cao, N., Fu, Y., & He, J. (2007). Mechanical properties of gelatin films cross-linked, respectively, by ferulic acid and tannin acid. *Food Hydrocolloids*, *21*(4), 575–584. https://doi.org/10.1016/j.foodhyd.2006.07.001

Chandrasekhar, J., Madhusudhan, M. C., & Raghavarao, K. S. M. S. (2012). Extraction of anthocyanins from red cabbage and purification using adsorption. *Food and Bioproducts Processing*, *90*(4), 615–623. https://doi.org/10.1016/j.fbp.2012.07.004

Chavoshizadeh, S., Pirsa, S., & Mohtarami, F. (2020). Sesame Oil Oxidation Control by Active and Smart Packaging System Using Wheat Gluten/Chlorophyll Film to Increase Shelf Life and Detecting Expiration Date. *European Journal of Lipid Science and Technology*, *122*(3), 1–12. https://doi.org/10.1002/ejlt.201900385

Chen, J. L., & Yan, X. P. (2011). Ionic strength and pH reversible response of visible and near-infrared fluorescence of graphene oxide nanosheets for monitoring the extracellular pH. *Chemical Communications*, *47*(11), 3135–3137. https://doi.org/10.1039/c0cc03999c

Choi, I., Lee, J. Y., Lacroix, M., & Han, J. (2017). Intelligent pH indicator film composed of agar/potato starch and anthocyanin extracts from purple sweet potato. *Food Chemistry*, *218*, 122–128. https://doi.org/10.1016/j.foodchem.2016.09.050

Cichello, S. A. (2015). Oxygen absorbers in food preservation: a review. *Journal of Food Science and Technology*, *52*(4), 1889–1895. https://doi.org/10.1007/s13197-014-1265-2

Coronado Jorge, M. F., Alexandre, E. M. C., Caicedo Flaker, C. H., Bittante, A. M. Q. B., & Sobral, P. J. D. A. (2015). Biodegradable films based on gelatin and montmorillonite produced by spreading. *International Journal of Polymer Science*, *2015*. https://doi.org/10.1155/2015/806791

Cortez, R., Luna-Vital, D. A., Margulis, D., & Gonzalez de Mejia, E. (2017). Natural Pigments: Stabilization Methods of Anthocyanins for Food Applications. *Comprehensive Reviews in Food Science and Food Safety*, *16*(1), 180–198. https://doi.org/10.1111/1541-4337.12244

Dainelli, D., Gontard, N., Spyropoulos, D., Zondervan-van den Beuken, E., & Tobback, P. (2008). Active and intelligent food packaging: legal aspects and safety concerns. *Trends in Food Science and Technology*, *19*(SUPPL. 1), S103–S112. https://doi.org/10.1016/j.tifs.2008.09.011

Dash, K. K., Deka, P., Bangar, S. P., Chaudhary, V., Trif, M., & Rusu, A. (2022). Applications of Inorganic Nanoparticles in Food Packaging: A Comprehensive Review. *Polymers*, *14*(3), 1–20. https://doi.org/10.3390/polym14030521

de Abreu, D. A. P., Cruz, J. M., & Losada, P. P. (2012). Active and Intelligent Packaging for the Food Industry. *Food Reviews International*, *28*(2), 146–187. https://doi.org/10.1080/87559129.2011.595022

de Oliveira Filho, J. G., Bertolo, M. R. V., Rodrigues, M. Á. V., Silva, G. da C., de Mendonça, G. M. N., Bogusz Junior, S., Ferreira, M. D., & Egea, M. B. (2022). Recent advances in the development of smart, active, and bioactive biodegradable biopolymer-based films containing betalains. *Food Chemistry*, *390*(January). https://doi.org/10.1016/j.foodchem.2022.133149

Delgado-Vargas, F., Jiménez, A. R., Paredes-López, O., & Francis, F. J. (2000).

Natural pigments: Carotenoids, anthocyanins, and betalains - Characteristics, biosynthesis, processing, and stability. In *Critical Reviews in Food Science and Nutrition* (Vol. 40, Issue 3). https://doi.org/10.1080/10408690091189257

Dhenadhayalan, N., Lin, K. C., Suresh, R., & Ramamurthy, P. (2016). Unravelling the Multiple Emissive States in Citric-Acid-Derived Carbon Dots. *Journal of Physical Chemistry C*, *120*(2), 1252–1261. https://doi.org/10.1021/acs.jpcc.5b08516

Dixit, A. M., Subba Rao, S. V., Article, O., Choudhary, K., Singh, M., Choudhary, O. P., Pillai, U., Samanta, J. N., Mandal, K., Saravanan, R., Gajbhiye, N. A., Ravi, V., Bhatia, A., Tripathi, T., Singh, S. C. S., Bisht, H., Behl, H. M., Roy, R., Sidhu, O. P., … Helmy, M. (2018). GENERAL STANDARD FOR THE LABELLING OF PREPACKAGED FOODS. *Analytical Biochemistry*, *11*(1), 1–5. http://link.springer.com/10.1007/978-3-319-59379-1%0Ahttp://dx.doi.org/10.1016/B978-0-12-420070-8.00002-7%0Ahttp://dx.doi.org/10.1016/j.ab.2015.03.024%0Ahttps://doi.org/10.1080/07352689.2018.1441103%0Ahttp://www.chile.bmw-motorrad.cl/sync/showroom/lam/es/

Dobrucka, R., & Cierpiszewski, R. (2014). Active and Intelligent Packaging Food – Research and Development – A Review. *Polish Journal of Food and Nutrition Sciences*, *64*(1), 7–15. https://doi.org/10.2478/v10222–012–0091–3

Drago, E., Campardelli, R., Pettinato, M., & Perego, P. (2020). Innovations in smart packaging concepts for food: An extensive review. *Foods*, *9*(11). https://doi.org/10.3390/foods9111628

Dutra Resem Brizio, A. P. (2016). Use of Indicators in Intelligent Food Packaging. In *Reference Module in Food Science* (pp. 1–5). Elsevier. https://doi.org/10.1016/B978-0-08-100596-5.03214-5

Etxabide, A., Uranga, J., Guerrero, P., & de la Caba, K. (2015). Improvement of barrier properties of fish gelatin films promoted bygelatin glycation with

lactose at high temperatures. *Lwt*, *63*(1), 315–321.
https://doi.org/10.1016/j.lwt.2015.03.079

European Union. (2009). Commission Regulation (EC) No. 450/2009 of 29 May
2009. *Official Journal of European Union*, *135*, 3–11. https://eur-
lex.europa.eu/LexUriServ/LexUriServ.do?uri=OJ:L:2009:135:0003:0011:EN:
PDF

Ezati, P., Tajik, H., Moradi, M., & Molaei, R. (2019). Intelligent pH-sensitive
indicator based on starch-cellulose and alizarin dye to track freshness of
rainbow trout fillet. *International Journal of Biological Macromolecules*, *132*,
157–165. https://doi.org/10.1016/j.ijbiomac.2019.03.173

FULEKI, T., & FRANCIS, F. J. (1968). Quantitative Methods for Anthocyanins. 2.
Determination of Total Anthocyanin and Degradation Index for Cranberry
Juice. *Journal of Food Science*, *33*(1), 78–83. https://doi.org/10.1111/j.1365-
2621.1968.tb00888.x

Gaikwad, K. K., Singh, S., & Ajji, A. (2019). Moisture absorbers for food
packaging applications. *Environmental Chemistry Letters*, *17*(2), 609–628.
https://doi.org/10.1007/s10311-018-0810-z

Ghaani, M., Cozzolino, C. A., Castelli, G., & Farris, S. (2016). An overview of the
intelligent packaging technologies in the food sector. *Trends in Food Science
and Technology*, *51*, 1–11. https://doi.org/10.1016/j.tifs.2016.02.008

Gokilamani, N., Muthukumarasamy, N., Thambidurai, M., Ranjitha, A., &
Velauthapillai, D. (2013). Utilization of natural anthocyanin pigments as
photosensitizers for dye-sensitized solar cells. *Journal of Sol-Gel Science and
Technology*, *66*(2), 212–219. https://doi.org/10.1007/s10971-013-2994-9

Gómez-Guillén, M. C., Pérez-Mateos, M., Gómez-Estaca, J., López-Caballero, E.,
Giménez, B., & Montero, P. (2009). Fish gelatin: a renewable material for
developing active biodegradable films. *Trends in Food Science and
Technology*, *20*(1), 3–16. https://doi.org/10.1016/j.tifs.2008.10.002

GONTARD, N., DUCHEZ, C., CUQ, J. -L, & GUILBERT, S. (1994). Edible composite films of wheat gluten and lipids: water vapour permeability and other physical properties. *International Journal of Food Science & Technology*, *29*(1), 39–50. https://doi.org/10.1111/j.1365-2621.1994.tb02045.x

Guo, J., Ge, L., Li, X., Mu, C., & Li, D. (2014). Periodate oxidation of xanthan gum and its crosslinking effects on gelatin-based edible films. *Food Hydrocolloids*, *39*, 243–250. https://doi.org/10.1016/j.foodhyd.2014.01.026

Hazaveh, P., Mohammadi Nafchi, A., & Abbaspour, H. (2015). The effects of sugars on moisture sorption isotherm and functional properties of cold water fish gelatin films. *International Journal of Biological Macromolecules*, *79*, 370–376. https://doi.org/10.1016/j.ijbiomac.2015.05.008

Heising, J. K., Dekker, M., Bartels, P. V., & (Tiny) Van Boekel, M. A. J. S. (2014). Monitoring the Quality of Perishable Foods: Opportunities for Intelligent Packaging. *Critical Reviews in Food Science and Nutrition*, *54*(5), 645–654. https://doi.org/10.1080/10408398.2011.600477

Hu, H., Yao, X., Qin, Y., Yong, H., & Liu, J. (2020). Development of multifunctional food packaging by incorporating betalains from vegetable amaranth (Amaranthus tricolor L.) into quaternary ammonium chitosan/fish gelatin blend films. *International Journal of Biological Macromolecules*, *159*, 675–684. https://doi.org/10.1016/j.ijbiomac.2020.05.103

Huang, X. W., Zou, X. B., Shi, J. Y., Guo, Y., Zhao, J. W., Zhang, J., & Hao, L. (2014). Determination of pork spoilage by colorimetric gas sensor array based on natural pigments. *Food Chemistry*, *145*, 549–554. https://doi.org/10.1016/j.foodchem.2013.08.101

Jeya Shakila, R., Jeevithan, E., Varatharajakumar, A., Jeyasekaran, G., & Sukumar, D. (2012). Comparison of the properties of multi-composite fish gelatin films with that of mammalian gelatin films. *Food Chemistry*, *135*(4), 2260–2267.

https://doi.org/10.1016/j.foodchem.2012.07.069

Jia, X., Li, J., & Wang, E. (2012). One-pot green synthesis of optically pH-sensitive carbon dots with upconversion luminescence. *Nanoscale*, *4*(18), 5572–5575. https://doi.org/10.1039/c2nr31319g

Jung, J., & Zhao, Y. (2016). Antimicrobial Packaging for Fresh and Minimally Processed Fruits and Vegetables. In *Antimicrobial Food Packaging*. Elsevier Inc. https://doi.org/10.1016/B978-0-12-800723-5.00018-8

Kalpana, S., Priyadarshini, S. R., Maria Leena, M., Moses, J. A., & Anandharamakrishnan, C. (2019). Intelligent packaging: Trends and applications in food systems. *Trends in Food Science and Technology*, *93*(October 2018), 145–157. https://doi.org/10.1016/j.tifs.2019.09.008

Kato, H., Tan, K. T., & Chai, D. (2010). Introduction. In *Barcodes for Mobile Devices* (pp. 1–10). Cambridge University Press. https://doi.org/10.1017/CBO9780511712241.002

Kchaou, H., Benbettaïeb, N., Jridi, M., Abdelhedi, O., Karbowiak, T., Brachais, C. H., Léonard, M. L., Debeaufort, F., & Nasri, M. (2018). Enhancement of structural, functional and antioxidant properties of fish gelatin films using Maillard reactions. *Food Hydrocolloids*, *83*, 326–339. https://doi.org/10.1016/j.foodhyd.2018.05.011

Kerry, J. P., O'Grady, M. N., & Hogan, S. A. (2006). Past, current and potential utilisation of active and intelligent packaging systems for meat and muscle-based products: A review. *Meat Science*, *74*(1), 113–130. https://doi.org/10.1016/j.meatsci.2006.04.024

Kilara, A. (2017). Regulatory aspects of yogurt. In *Yogurt in Health and Disease Prevention*. Elsevier Inc. https://doi.org/10.1016/B978-0-12-805134-4.00006-7

Kurek, M., Garofulić, I. E., Bakić, M. T., Ščetar, M., Uzelac, V. D., & Galić, K.

(2018). Development and evaluation of a novel antioxidant and pH indicator film based on chitosan and food waste sources of antioxidants. *Food Hydrocolloids*, *84*(May), 238–246. https://doi.org/10.1016/j.foodhyd.2018.05.050

Kuswandi, B., Jayus, Oktaviana, R., Abdullah, A., & Heng, L. Y. (2014). A Novel On-Package Sticker Sensor Based on Methyl Red for Real-Time Monitoring of Broiler Chicken Cut Freshness. *Packaging Technology and Science*, *27*(1), 69–81. https://doi.org/10.1002/pts.2016

Kuswandi, B., Jayus, Restyana, A., Abdullah, A., Heng, L. Y., & Ahmad, M. (2012). A novel colorimetric food package label for fish spoilage based on polyaniline film. *Food Control*, *25*(1), 184–189. https://doi.org/10.1016/j.foodcont.2011.10.008

Kuswandi, B., Wicaksono, Y., Jayus, Abdullah, A., Heng, L. Y., & Ahmad, M. (2011). Smart packaging: Sensors for monitoring of food quality and safety. *Sensing and Instrumentation for Food Quality and Safety*, *5*(3–4), 137–146. https://doi.org/10.1007/s11694-011-9120-x

Lagarón, J. M., Cabedo, L., Cava, D., Feijoo, J. L., Gavara, R., & Gimenez, E. (2005). Improving packaged food quality and safety. Part 2: Nanocomposites. *Food Additives and Contaminants*, *22*(10), 994–998. https://doi.org/10.1080/02652030500239656

Latos-Brozio, M., & Masek, A. (2020). The application of natural food colorants as indicator substances in intelligent biodegradable packaging materials. *Food and Chemical Toxicology*, *135*(June 2019), 110975. https://doi.org/10.1016/j.fct.2019.110975

Lee, D. S., Wang, H. J., Jaisan, C., & An, D. S. (2022). Active food packaging to control carbon dioxide. *Packaging Technology and Science*, *35*(3), 213–227. https://doi.org/10.1002/pts.2627

Lee, J.-E., & Kim, K. M. (2010). Characteristics of soy protein isolate-

montmorillonite composite films. *Journal of Applied Polymer Science*, *116*(5), n/a-n/a. https://doi.org/10.1002/app.31316

Lee, S. Y., Lee, S. J., Choi, D. S., & Hur, S. J. (2015). Current topics in active and intelligent food packaging for preservation of fresh foods. *Journal of the Science of Food and Agriculture*, *95*(14), 2799–2810. https://doi.org/10.1002/jsfa.7218

Li, Y., Chen, H., Dong, Y., Li, K., Li, L., & Li, J. (2016). Carbon nanoparticles/soy protein isolate bio-films with excellent mechanical and water barrier properties. *Industrial Crops and Products*, *82*, 133–140. https://doi.org/10.1016/j.indcrop.2015.11.072

Liang, T., Sun, G., Cao, L., Li, J., & Wang, L. (2019). A pH and NH3 sensing intelligent film based on Artemisia sphaerocephala Krasch. gum and red cabbage anthocyanins anchored by carboxymethyl cellulose sodium added as a host complex. *Food Hydrocolloids*, *87*(August 2018), 858–868. https://doi.org/10.1016/j.foodhyd.2018.08.028

Liu, X., Li, H. B., Shi, L., Meng, X., Wang, Y., Chen, X., Xu, H., Zhang, W., Fang, X., & Ding, T. (2017). Structure and photoluminescence evolution of nanodots during pyrolysis of citric acid: From molecular nanoclusters to carbogenic nanoparticles. *Journal of Materials Chemistry C*, *5*(39), 10302–10312. https://doi.org/10.1039/c7tc03429f

Liu, J., Wang, H., Wang, P., Guo, M., Jiang, S., Li, X., & Jiang, S. (2018). Films based on κ-carrageenan incorporated with curcumin for freshness monitoring. *Food Hydrocolloids*, *83*, 134–142. https://doi.org/10.1016/j.foodhyd.2018.05.012

Lu, Y., Luo, Q., Chu, Y., Tao, N., Deng, S., Wang, L., & Li, L. (2022). Application of Gelatin in Food Packaging: A Review. *Polymers*, *14*(3). https://doi.org/10.3390/polym14030436

Ludmerczki, R., Mura, S., Carbonaro, C. M., Mandity, I. M., Carraro, M., Senes,

N., Garroni, S., Granozzi, G., Calvillo, L., Marras, S., Malfatti, L., & Innocenzi, P. (2019). Carbon Dots from Citric Acid and its Intermediates Formed by Thermal Decomposition. *Chemistry - A European Journal*, *25*(51), 11963–11974. https://doi.org/10.1002/chem.201902497

Ma, Z., Chen, P., Cheng, W., Yan, K., Pan, L., Shi, Y., & Yu, G. (2018). Highly Sensitive, Printable Nanostructured Conductive Polymer Wireless Sensor for Food Spoilage Detection. *Nano Letters*, *18*(7), 4570–4575. https://doi.org/10.1021/acs.nanolett.8b01825

MacIel, V. B. V., Franco, T. T., & Yoshida, C. M. P. (2012). Alternative intelligent material for packaging using chitosan films as colorimetric temperature indicators. *Polimeros*, *22*(4), 318–324. https://doi.org/10.1590/S0104-14282012005000054

Masutani, E. M., Kinoshita, C. K., Tanaka, T. T., Ellison, A. K. D., & Yoza, B. A. (2014). Increasing thermal stability of gelatin by UV-induced cross-linking with glucose. International Journal of Biomaterials, 2014. https://doi.org/10.1155/2014/979636

Mchugh, T. H., Avena-bustillos, F. L., & Krochta, J. M. (1993). Hydrophilic Edible Films : Modified Procedure for Water Vapor Permeability and Explanation of Thickness Effects. *Journal of Food Science*, *58*(4), 899–903. https://doi.org/https://doi.org/10.1111/j.1365-2621.1993.tb09387.x

McHUGH, T. H., AVENA-BUSTILLOS, R., & KROCHTA, J. M. (1993). Hydrophilic Edible Films: Modified Procedure for Water Vapor Permeability and Explanation of Thickness Effects. *Journal of Food Science*, *58*(4), 899–903. https://doi.org/10.1111/j.1365-2621.1993.tb09387.x

Mexis, S. F., & Kontominas, M. G. (2014). Packaging: Active Food Packaging. In *Encyclopedia of Food Microbiology: Second Edition* (Second Edi, Vol. 2). Elsevier. https://doi.org/10.1016/B978-0-12-384730-0.00434-1

Michelmore, A. (2016). Thin film growth on biomaterial surfaces. In *Thin Film*

Coatings for Biomaterials and Biomedical Applications. Elsevier Ltd.
https://doi.org/10.1016/b978-1-78242-453-6.00002-x

Moradi, M., Tajik, H., Almasi, H., Forough, M., & Ezati, P. (2019). A novel pH-sensing indicator based on bacterial cellulose nanofibers and black carrot anthocyanins for monitoring fish freshness. *Carbohydrate Polymers*, *222*(June), 115030. https://doi.org/10.1016/j.carbpol.2019.115030

Mortensen, A. (2006). Carotenoids and other pigments as natural colorants. *Pure and Applied Chemistry*, *78*(8), 1477–1491. https://doi.org/10.1351/pac200678081477

Musso, Y. S., Salgado, P. R., & Mauri, A. N. (2017). Smart edible films based on gelatin and curcumin. *Food Hydrocolloids*, *66*, 8–15. https://doi.org/10.1016/j.foodhyd.2016.11.007

Musso, Y. S., Salgado, P. R., & Mauri, A. N. (2019). Smart gelatin films prepared using red cabbage (Brassica oleracea L.) extracts as solvent. *Food Hydrocolloids*, *89*(November 2018), 674–681. https://doi.org/10.1016/j.foodhyd.2018.11.036

Müller, P., & Schmid, M. (2019). Intelligent packaging in the food sector: A brief overview. *Foods*, *8*(1). https://doi.org/10.3390/foods8010016

Naghdi, S., Rezaei, M., & Abdollahi, M. (2021). A starch-based pH-sensing and ammonia detector film containing betacyanin of paperflower for application in intelligent packaging of fish. *International Journal of Biological Macromolecules*, *191*(February), 161–170. https://doi.org/10.1016/j.ijbiomac.2021.09.045

Naseer, S., Hussain, S., & Abid, A. (2019). Betalain as a food colorant: Its sources, chemistry and health benefits. *Proceedings of the Pakistan Academy of Sciences: Part B*, *56*(2), 1–8.

Nilsuwan, K., Benjakul, S., & Prodpran, T. (2018). Properties and antioxidative

activity of fish gelatin-based film incorporated with epigallocatechin gallate. *Food Hydrocolloids*, *80*, 212–221. https://doi.org/10.1016/j.foodhyd.2018.01.033

Nor Adilah, A., Gun Hean, C., & Nur Hanani, Z. A. (2021). Incorporation of graphene oxide to enhance fish gelatin as bio-packaging material. *Food Packaging and Shelf Life*, *28*(May 2020), 100679. https://doi.org/10.1016/j.fpsl.2021.100679

Otoni, C. G., Avena-Bustillos, R. J., Chiou, B. Sen, Bilbao-Sainz, C., Bechtel, P. J., & McHugh, T. H. (2012). Ultraviolet-B Radiation Induced Cross-linking Improves Physical Properties of Cold- and Warm-Water Fish Gelatin Gels and Films. *Journal of Food Science*, *77*(9), 215–223. https://doi.org/10.1111/j.1750-3841.2012.02839.x

Pereira, V. A., de Arruda, I. N. Q., & Stefani, R. (2015). Active chitosan/PVA films with anthocyanins from Brassica oleraceae (Red Cabbage) as Time-Temperature Indicators for application in intelligent food packaging. *Food Hydrocolloids*, *43*, 180–188. https://doi.org/10.1016/j.foodhyd.2014.05.014

Prietto, L., Mirapalhete, T. C., Pinto, V. Z., Hoffmann, J. F., Vanier, N. L., Lim, L. T., Guerra Dias, A. R., & da Rosa Zavareze, E. (2017). pH-sensitive films containing anthocyanins extracted from black bean seed coat and red cabbage. *LWT - Food Science and Technology*, *80*, 492–500. https://doi.org/10.1016/j.lwt.2017.03.006

Priyadarshi, R., Ezati, P., & Rhim, J. W. (2021). Recent Advances in Intelligent Food Packaging Applications Using Natural Food Colorants. *ACS Food Science and Technology*, *1*(2), 124–138. https://doi.org/10.1021/acsfoodscitech.0c00039

Qin, Y., Liu, Y., Zhang, X., & Liu, J. (2020). Development of active and intelligent packaging by incorporating betalains from red pitaya (Hylocereus polyrhizus) peel into starch/polyvinyl alcohol films. *Food Hydrocolloids*, *100*(August

2019), 105410. https://doi.org/10.1016/j.foodhyd.2019.105410

Ramamoorthy, R., Radha, N., Maheswari, G., Anandan, S., Manoharan, S., & Victor Williams, R. (2016). Betalain and anthocyanin dye-sensitized solar cells. *Journal of Applied Electrochemistry*, *46*(9), 929–941. https://doi.org/10.1007/s10800-016-0974-9

Rani, S., Kumar, K. D., Mandal, S., & Kumar, R. (2020). Functionalized carbon dot nanoparticles reinforced soy protein isolate biopolymeric film. *Journal of Polymer Research*, *27*(10), 1–10. https://doi.org/10.1007/s10965-020-02276-1

Realini, C. E., & Marcos, B. (2014). Active and intelligent packaging systems for a modern society. *Meat Science*, *98*(3), 404–419. https://doi.org/10.1016/j.meatsci.2014.06.031

Reddy, N., Li, Y., & Yang, Y. (2009). Alkali-catalyzed low temperature wet crosslinking of plant proteins using carboxylic acids. *Biotechnology Progress*, *25*(1), 139–146. https://doi.org/10.1002/btpr.86

Rehman, A., Tong, Q., Jafari, S. M., Assadpour, E., Shehzad, Q., Aadil, R. M., Iqbal, M. W., Rashed, M. M. A., Mushtaq, B. S., & Ashraf, W. (2020). Carotenoid-loaded nanocarriers: A comprehensive review. *Advances in Colloid and Interface Science*, *275*, 102048. https://doi.org/10.1016/j.cis.2019.102048

Rezaee, M., Askari, G., EmamDjomeh, Z., & Salami, M. (2020). UV-irradiated gelatin-chitosan bio-based composite film, physiochemical features and release properties for packaging applications. *International Journal of Biological Macromolecules*, *147*, 990–996. https://doi.org/10.1016/j.ijbiomac.2019.10.066

Rhim, J. W., Gennadios, A., Fu, D., Weller, C. L., & Hanna, M. A. (1999). Properties of ultraviolet irradiated protein films. *LWT - Food Science and Technology*, *32*(3), 129–133. https://doi.org/10.1006/fstl.1998.0516

Rhim, J. W., & Ng, P. K. W. (2007). Natural biopolymer-based nanocomposite films for packaging applications. *Critical Reviews in Food Science and Nutrition*, *47*(4), 411–433. https://doi.org/10.1080/10408390600846366

Roco, M. C. (2003). Nanotechnology: Convergence with modern biology and medicine. *Current Opinion in Biotechnology*, *14*(3), 337–346. https://doi.org/10.1016/S0958-1669(03)00068-5

Roy, S., Ezati, P., & Rhim, J. W. (2021). Gelatin/Carrageenan-Based Functional Films with Carbon Dots from Enoki Mushroom for Active Food Packaging Applications. *ACS Applied Polymer Materials*, *3*(12), 6437–6445. https://doi.org/10.1021/acsapm.1c01175

Rukchon, C., Nopwinyuwong, A., Trevanich, S., Jinkarn, T., & Suppakul, P. (2014). Development of a food spoilage indicator for monitoring freshness of skinless chicken breast. *Talanta*, *130*, 547–554. https://doi.org/10.1016/j.talanta.2014.07.048

Sadeghi, K., Shahedi, M., Najafi, M., Sadeghi, A., & Shirani, M. (2021). Types of nanomaterials in food packaging: A review. *International Journal of Nanoparticles*, *13*(2), 63–95. https://doi.org/10.1504/IJNP.2021.116770

Sajkiewicz, P., & Kolbuk, D. (2014). Electrospinning of gelatin for tissue engineering-molecular conformation as one of the overlooked problems. *Journal of Biomaterials Science, Polymer Edition*, *25*(18), 2009–2022. https://doi.org/10.1080/09205063.2014.975392

Salgado, P. R., Di Giorgio, L., Musso, Y. S., & Mauri, A. N. (2021). Recent Developments in Smart Food Packaging Focused on Biobased and Biodegradable Polymers. *Frontiers in Sustainable Food Systems*, *5*(April), 1–30. https://doi.org/10.3389/fsufs.2021.630393

Santos-Zea, L., Villera-Castrejón, J., & Gutiérrez-Uribe, J. (2019). Bound phenolics in food-Reference series in phytochemistry. In *Bioactive Molecules in Food* (Issue September 2018). http://link.springer.com/10.1007/978-3-319-

78030-6

Schaefer, D., & Cheung, W. M. (2018). Smart Packaging: Opportunities and
Challenges. *Procedia CIRP*, *72*, 1022–1027.
https://doi.org/10.1016/j.procir.2018.03.240

Schmidt, D., Shah, D., & Giannelis, E. P. (2002). New advances in
polymer/layered silicate nanocomposites. *Current Opinion in Solid State and
Materials Science*, *6*(3), 205–212. https://doi.org/10.1016/S1359-
0286(02)00049-9

Selman, J. D. (1995). Time—temperature indicators. In *Active Food Packaging*
(pp. 215–237). Springer US. https://doi.org/10.1007/978-1-4615-2175-4_10

Shao, P., Liu, L., Yu, J., Lin, Y., Gao, H., Chen, H., & Sun, P. (2021). An overview
of intelligent freshness indicator packaging for food quality and safety
monitoring. *Trends in Food Science and Technology*, *118*(PA), 285–296.
https://doi.org/10.1016/j.tifs.2021.10.012

Sharma, L., Sharma, H. K., & Saini, C. S. (2018). Edible films developed from
carboxylic acid cross-linked sesame protein isolate: barrier, mechanical, thermal,
crystalline and morphological properties. Journal of Food Science and Technology,
55(2), 532–539. https://doi.org/10.1007/s13197-017-2962-4

Singh, S., Gaikwad, K. K., & Lee, Y. S. (2018). Anthocyanin – A Natural Dye for
Smart Food Packaging Systems. *KOREAN JOURNAL OF PACKAGING
SCIENCE AND TECHNOLOGY*, *24*(3), 167–180.
https://doi.org/10.20909/kopast.2018.24.3.167

Smeriglio, A., Barreca, D., Bellocco, E., & Trombetta, D. (2016). Chemistry,
Pharmacology and Health Benefits of Anthocyanins. *Phytotherapy Research*,
1286(April), 1265–1286. https://doi.org/10.1002/ptr.5642

Sorrentino, A., Gorrasi, G., & Vittoria, V. (2007). Potential perspectives of bio-
nanocomposites for food packaging applications. *Trends in Food Science and*

Technology, *18*(2), 84–95. https://doi.org/10.1016/j.tifs.2006.09.004

Tajeddin, B., & Arabkhedri, M. (2020). Polymers and food packaging. In *Polymer Science and Innovative Applications*. INC. https://doi.org/10.1016/b978-0-12-816808-0.00016-0

Taoukis, P. S., & Labuza, T. P. (2003). Time-temperature indicators (TTIs). In *Novel Food Packaging Techniques*. Woodhead Publishing Limited. https://doi.org/10.1533/9781855737020.1.103

TAOUKIS, P. S., & LABUZA, T. P. (1989). Applicability of Time-Temperature Indicators as Shelf Life Monitors of Food Products. *Journal of Food Science*, *54*(4), 783–788. https://doi.org/10.1111/j.1365-2621.1989.tb07882.x

Thostenson, E. T., Li, C., & Chou, T. W. (2005). Nanocomposites in context. *Composites Science and Technology*, *65*(3–4), 491–516. https://doi.org/10.1016/j.compscitech.2004.11.003

Uranga, J., Leceta, I., Etxabide, A., Guerrero, P., & De La Caba, K. (2016). Cross-linking of fish gelatins to develop sustainable films with enhanced properties. *European Polymer Journal*, *78*, 82–90. https://doi.org/10.1016/j.eurpolymj.2016.03.017

Vanderroost, M., Ragaert, P., Devlieghere, F., & De Meulenaer, B. (2014). Intelligent food packaging: The next generation. *Trends in Food Science and Technology*, *39*(1), 47–62. https://doi.org/10.1016/j.tifs.2014.06.009

Villaño, D., García-Viguera, C., & Mena, P. (2015). Colors: Health Effects. *Encyclopedia of Food and Health*, 265–272. https://doi.org/10.1016/B978-0-12-384947-2.00190-2

Vinha, A. F., Rodrigues, F., Nunes, M. A., & Oliveira, M. B. P. P. (2018). Natural pigments and colorants in foods and beverages. In *Polyphenols: Properties, Recovery, and Applications*. Elsevier Inc. https://doi.org/10.1016/B978-0-12-813572-3.00011-7

Walsh, T. (2011). The Plastic Piping Industry in North America. In *Applied Plastics Engineering Handbook*. Elsevier. https://doi.org/10.1016/B978-1-4377-3514-7.10034-0

Wan, C., Frydrych, M., & Chen, B. (2011). Strong and bioactive gelatin-graphene oxide nanocomposites. *Soft Matter*, *7*(13), 6159–6166. https://doi.org/10.1039/c1sm05321c

Wang, R., Lu, K. Q., Tang, Z. R., & Xu, Y. J. (2017). Recent progress in carbon quantum dots: synthesis, properties and applications in photocatalysis. *Journal of Materials Chemistry A*, *5*(8), 3717–3734. https://doi.org/10.1039/c6ta08660h

Wrolstad, R. E., & Culver, C. A. (2012). Alternatives to those artificial FD & C food colorants. *Annual Review of Food Science and Technology*, *3*(1), 59–77. https://doi.org/10.1146/annurev-food-022811-101118

Xu, H., Yang, X., Li, G., Zhao, C., & Liao, X. (2015). Green Synthesis of Fluorescent Carbon Dots for Selective Detection of Tartrazine in Food Samples. *Journal of Agricultural and Food Chemistry*, *63*(30), 6707–6714. https://doi.org/10.1021/acs.jafc.5b02319

Yam, K. L. (2012). Intelligent packaging to enhance food safety and quality. In *Emerging Food Packaging Technologies* (Issue 2005). Woodhead Publishing Limited. https://doi.org/10.1533/9780857095664.2.137

Yildirim, S., Röcker, B., Pettersen, M. K., Nilsen-Nygaard, J., Ayhan, Z., Rutkaite, R., Radusin, T., Suminska, P., Marcos, B., & Coma, V. (2018). Active Packaging Applications for Food. *Comprehensive Reviews in Food Science and Food Safety*, *17*(1), 165–199. https://doi.org/10.1111/1541-4337.12322

Yildiz, E., Sumnu, G., & Kahyaoglu, L. N. (2021). Monitoring freshness of chicken breast by using natural halochromic curcumin loaded chitosan/PEO nanofibers as an intelligent package. *International Journal of Biological Macromolecules*, *170*, 437–446.

https://doi.org/10.1016/j.ijbiomac.2020.12.160

Young, E., Mirosa, M., & Bremer, P. (2020). A systematic review of consumer perceptions of smart packaging technologies for food. *Frontiers in Sustainable Food Systems*, *4*(May), 1–20. https://doi.org/10.3389/fsufs.2020.00063

Yu, Y., Li, C., Chen, C., Huang, H., Liang, C., Lou, Y., Chen, X. B., Shi, Z., & Feng, S. (2019). Saccharomyces-derived carbon dots for biosensing pH and vitamin B 12. *Talanta*, *195*(November 2018), 117–126. https://doi.org/10.1016/j.talanta.2018.11.010

Zhai, X., Shi, J., Zou, X., Wang, S., Jiang, C., Zhang, J., Huang, X., Zhang, W., & Holmes, M. (2017). Novel colorimetric films based on starch/polyvinyl alcohol incorporated with roselle anthocyanins for fish freshness monitoring. *Food Hydrocolloids*, *69*, 308–317. https://doi.org/10.1016/j.foodhyd.2017.02.014

Zhang, C., Yin, A. X., Jiang, R., Rong, J., Dong, L., Zhao, T., Sun, L. D., Wang, J., Chen, X., & Yan, C. H. (2013). Time-temperature indicator for perishable products based on kinetically programmable Ag overgrowth on Au nanorods. *ACS Nano*, *7*(5), 4561–4568. https://doi.org/10.1021/nn401266u

Zhang, J., Zou, X., Zhai, X., Huang, X. W., Jiang, C., & Holmes, M. (2019). Preparation of an intelligent pH film based on biodegradable polymers and roselle anthocyanins for monitoring pork freshness. *Food Chemistry*, *272*(August 2018), 306–312. https://doi.org/10.1016/j.foodchem.2018.08.041

Zin, M. M., Anucha, C. B., & Bánvölgyi, S. (2020). Recovery of Phytochemicals via Electromagnetic. *Foods*, *9*(918), 1–20. 10.3390/foods9070918

APPENDICES

A. Statistical Analysis

Table1: The percent relative crystallinity of FG films

	N Analysis	N Missing	Mean	Standard Deviation	SE of Mean
FG	2.00	0.00	14.53	0.25	0.18
FG-UV	2.00	0.00	14.84	0.12	0.08
FG-UV-25	2.00	0.00	14.07	0.14	0.10
FG-UV-50	2.00	0.00	13.67	0.46	0.33
FG-UV-100	2.00	0.00	13.09	0.06	0.04

	DF	Sum of Squares	Mean Square	F Value	Prob>F
Model	4	3.83226	0.95807	15.2704	0.00521
Error	5	0.3137	0.06274		
Total	9	4.14596			

At the 0.05 level. the population means are significantly different

R-Square	Coeff Var	Root MSE	Data Mean
0.92434	0.01784	0.25048	14.038

Tukey Test

	Mean	Groups		
FG	14.835	A		
FG-UV	14.53	A	B	
FG-UV-25	14.07	A	B	C
FG-UV-50	13.665		B	C
FG-UV-100	13.09			C

Means that do not share a letter are significantly different.

Table 2: Water solubility of FG films

	N Analysis	N Missing	Mean	Standard Deviation	SE of Mean
FG	3.0	0.0	82.3	3.4	1.9
FG-UV	3.0	0.0	63.5	3.4	2.0
FG-UV-25	3.0	0.0	56.2	1.6	0.9
FG-UV-50	3.0	0.0	49.8	2.8	1.6
FG-UV-100	3.0	0.0	38.8	2.2	1.3

	DF	Sum of Squares	Mean Square	F Value	Prob>F
Model	4	3183.3	795.8	104.9	0
Error	10	75.9	7.6		
Total	14	3259.1			

At the 0.05 level, the population means are significantly different

R-Square	Coeff Var	Root MSE	Data Mean
1.0	0.0	2.8	58.1

Tukey Test

	Mean	Groups			
FG	82.3	A			
FG-UV	63.5		B		
FG-UV-25	56.2		B	C	
FG-UV-50	49.8			C	
FG-UV-100	38.8				D

Table 3: Tensile strength of FG films

	N Analysis	N Missing	Mean	Standard Deviation	SE of Mean
FG	2	0	22.6	0.6	0.4
FG-UV	2	0	30.7	0.6	0.4
FG-UV-25	2	0	34.5	1.1	0.8
FG-UV-50	2	0	34.9	1.5	1
FG-UV-100	2	0	36.9	0.4	0.3

	DF	Sum of Squares	Mean Square	F Value	Prob>F
Model	4.0	256.3	64.1	74.8	0.0
Error	5.0	4.3	0.9		
Total	9.0	260.6			

At the 0.05 level. the population means are significantly different.

R-Square	Coeff Var	Root MSE	Data Mean
1.0	0.0	0.9	31.9

Tukey Test

	Mean	Groups		
FG	36.9	A		
FG-UV	34.9	A		
FG-UV-25	34.5	A		
FG-UV-50	30.7		B	
FG-UV-100	22.6			C

Means that do not share a letter are significantly different.

Table 4: Elongation at break of FG films

	N Analysis	N Missing	Mean	Standard Deviation	SE of Mean
FG	2	0	223.15525	20.15997	14.25525
FG-UV	2	0	117.806	4.2087	2.976
FG-UV-25	2	0	136.807	5.76009	4.073
FG-UV-50	2	0	124.244	8.11051	5.735
FG-UV-100	2	0	120.668	1.86959	1.322

	DF	Sum of Squares	Mean Square	F Value	Prob>F
Model	4	15873.327	3968.33175	37.67938	6.3179E-4
Error	5	526.59193	105.31839		
Total	9	16399.91893			

R-Square	Coeff Var	Root MSE	Data Mean
0.96789	0.071	10.26247	144.53605

Tukey Test

	Mean	Groups	
FG	223.2	A	
FG-UV	136.8		B
FG-UV-25	124.2		B
FG-UV-50	120.7		B
FG-UV-100	117.8		B

Means that do not share a letter are significantly different.

Table 5: FG film thickness

	N Analysis	N Missing	Mean	Standard Deviation	SE of Mean
FG	2	0	0.1875	0.01061	0.0075
FG-UV	2	0	0.1665	0.01909	0.0135
FG-UV-25	2	0	0.1575	0.01061	0.0075
FG-UV-50	2	0	0.165	0.00707	0.005
FG-UV-100	2	0	0.195	0.00707	0.005

	DF	Sum of Squares	Mean Square	F Value	Prob>F
Model	4	0.00206	5.1615E-4	3.74293	0.09013
Error	5	6.895E-4	1.379E-4		
Total	9	0.00275			

R-Square	Coeff Var	Root MSE	Data Mean
0.74965	0.06737	0.01174	0.1743

Tukey Test

	Mean	Groups
FG-UV-100	0.195	A
FG	0.1875	A
FG-UV	0.1665	A
FG-UV-50	0.165	A
FG-UV-25	0.1575	A

Table 6: WVP of FG films

	N Analysis	N Missing	Mean	Standard Deviation	SE of Mean
FG	2.00	0.00	7.12	1.10	0.77
FG-UV	2.00	0.00	5.32	0.21	0.15
FG-UV-25	2.00	0.00	4.57	0.30	0.21
FG-UV-50	2.00	0.00	4.53	0.04	0.02
FG-UV-100	2.00	0.00	2.97	0.07	0.05

	DF	Sum of Squares	Mean Square	F Value	Prob>F
Model	4.00	18.12	4.53	16.93	0.00
Error	5.00	1.34	0.27		
Total	9.00	19.46			

R-Square	Coeff Var	Root MSE	Data Mean
0.93	0.11	0.52	4.90

Tukey Test

	Mean	Groups		
FG	7.12	A		
FG-UV	5.32	A	B	
FG-UV-25	4.57		B	C
FG-UV-50	4.53		B	C
FG-UV-100	2.97			C

Means that do not share a letter are significantly different.

Table 7: TVB-N

	N Analysis	N Missing	Mean	Standard Deviation	SE of Mean
1. Day	2.00	0.00	11.26	0.40	0.28
2. Day	2.00	0.00	12.14	0.26	0.19
3. Day	2.00	0.00	12.96	0.66	0.47
4. Day	2.00	0.00	14.46	0.13	0.09
5. Day	2.00	0.00	16.61	0.98	0.70
6. Day	2.00	0.00	21.92	2.31	1.63
7. Day	2.00	0.00	30.24	1.98	1.40
8. Day	2.00	0.00	41.62	3.96	2.80
9. Day	2.00	0.00	44.14	6.99	4.94

	DF	Sum of Squares	Mean Square	F Value	Prob>F
Model	8.00	2634.19	329.27	39.28	0.00
Error	9.00	75.45	8.38		
Total	17.00	2709.65			

At the 0.05 level. the population means are significantly different.

R-Square	Coeff Var	Root MSE	Data Mean
0.97	0.13	2.90	22.82

Tukey Test

	Mean	Groups			
9. Day	44.14	A			
8. Day	41.62	A	B		
7. Day	30.24		B	C	
6. Day	21.92			C	D
5. Day	16.61				D
4. Day	14.46				D
3. Day	12.96				D
2. Day	12.14				D
1. Day	11.26				D

Means that do not share a letter are significantly different.

Table 8: Correlation between the TVB-N and TVC values during chicken spoilage trails

TVB-N	TVC	r
11.30	2.48	0.91
12.14	2.72	
12.96	3.18	
14.50	4.39	
16.60	4.97	
21.90	6.66	
30.20	7.22	
41.62	7.37	
44.14	8.24	

Regression Statistics	
Multiple R	0.91
R Square	0.83
Adjusted R Square	0.81
Standard Error	0.97
Observations	9

ANOVA

	df	SS	MS	F	Significance F
Regression	1	32.0115	32.0115	34.3796	0.0006
Residual	7	6.5178	0.9311		
Total	8	38.5294			

	Coefficients	Standart Error	t Stat	P-value	Lower %95	Upper %95	Lower 95,0%	Upper 95,0%
Intecept	1.6871	0.6871	2.4556	0.0437	0.0625	3.3118	0.0625	3.3118
TVB-N	0.1560	0.0266	5.8634	0.0006	0.0931	0.2189	0.0931	0.2189